Ignition delay times of NH_3 /DME blends at high pressure and low DME fraction

RCM experiments and simulations

Dai, Liming; Hashemi, Hamid; Glarborg, Peter; Gersen, Sander; Marshall, Paul; Mokhov, Anatoli; Levinsky, Howard

Published in:
Combustion and Flame

Link to article, DOI:
10.1016/j.combustflame.2020.12.048

Publication date:
2021

Document Version
Peer reviewed version

Ignition delay times of NH_3 /DME blends at high pressure and low DME fraction: RCM experiments and simulations

Liming Dai[a], Hamid Hashemi[b], Peter Glarborg[b], Sander Gersen[c], Paul Marshall[d], Anatoli Mokhov[a] and Howard Levinsky[a*]

[a]Energy and Sustainability Research Institute, University of Groningen, Nijenborgh 6, 9747 AG Groningen, The Netherlands

[b]Department of Chemical and Biochemical Engineering, Technical University of Denmark, Kgs. Lyngby DK-2800, Denmark

[c]DNV GL Oil & Gas, P.O. Box 2029, 9704 CA Groningen, The Netherlands

[d]Department of Chemistry and Center for Advanced Scientific Computing and Modeling, University of North Texas, 1155 Union Circle #305070, Denton, Texas, 76203-5017

*Corresponding author: Howard Levinsky
Energy and Sustainability Research Institute
University of Groningen,
Nijenborgh 6
9747 AG Groningen, The Netherlands

Email: h.b.levinsky@rug.nl

Ignition delay times of NH_3 /DME blends at high pressure and low DME fraction: RCM experiments and simulations

Liming Dai[a], Hamid Hashemi[b], Peter Glarborg[b], Sander Gersen[c], Paul Marshall[d], Anatoli Mokhov[a] and Howard Levinsky[a*]

[a]Energy and Sustainability Research Institute, University of Groningen, Nijenborgh 6, 9747 AG Groningen, The Netherlands

[b]Department of Chemical and Biochemical Engineering, Technical University of Denmark, Kgs. Lyngby DK-2800, Denmark

[c]DNV GL Oil & Gas, P.O. Box 2029, 9704 CA Groningen, The Netherlands

[d]Department of Chemistry and Center for Advanced Scientific Computing and Modeling, University of North Texas, 1155 Union Circle #305070, Denton, Texas, 76203-5017

Abstract

Autoignition delay times of ammonia/dimethyl ether (NH_3/DME) mixtures were measured in a rapid compression machine with DME fractions of 0, 2 and 5 and 100% in the fuel. The measurements were performed at equivalence ratios φ=0.5, 1.0 and 2.0 and pressures in the range 10-70 bar; depending on the fuel composition, the temperatures after compression varied from 610 K to 1180 K. Admixture of DME is seen to have a dramatic effect on the ignition delay time, effectively shifting the curves of ignition delay vs. temperature to lower temperatures, up to ~250 K compared to pure ammonia. Two-stage ignition is observed at φ=1.0 and 2.0 with 2% and 5% DME in the fuel, despite the pressure being higher than that at which pure DME shows two-stage ignition. At φ=0.5, a reproducible pre-ignition pressure rise is observed for both DME fractions, which is not observed in the pure fuel components. A novel NH_3/DME mechanism was developed, including modifications in the NH_3 subset and addition of the NH_2+CH_3OCH_3 reaction, with rate coefficients calculated from ab initio theory. Simulations faithfully reproduce the observed pre-ignition pressure rise. While the mechanism also exhibits two-stage ignition for NH_3/DME mixtures, both qualitative and quantitative improvement is recommended. The overall ignition delay times for ammonia/DME mixtures are predicted well, generally being within 50% of the experimental values, although reduced performance is observed for pure ammonia at φ=2.0. Simulating the ignition process, we observe that the DME is oxidized much more rapidly than ammonia. Analysis of the mechanism indicates that this 'early DME oxidation' generates reactive species that initiate the oxidation of ammonia, which in turn begins heat release that raises the temperature and accelerates the oxidation process towards ignition. The reaction path analysis shows that the low-temperature chain-branching reactions of DME are important in the early oxidation of the fuel, while the sensitivity analysis indicates that several reactions in the oxidation of DME, including cross reactions between DME and NH_3 species presented here, are critical to ignition, even at fractions of 2% DME in the fuel.

Key words: ammonia/DME ignition, ignition enhancement, pre-ignition heat release, RCM measurements

1. Introduction

There is growing interest in ammonia (NH_3) as an alternative fuel in combustion engines to reduce greenhouse emissions currently produced by using fossil fuels. Historically, ammonia has been used as an engine fuel in, among others, buses in Belgium during World War II [1] and in the X-15 test plane 1950s [2]. However, compared to conventional fossil fuels, ammonia has a much lower burning velocity [3,4] and higher autoignition temperature [4], which prevents the use of ammonia as a pure fuel in existing engines. Using other compounds as 'additives' to enhance combustion to the point that the ammonia/additive mixture performs comparably with the existing fuel (see for example, [4–6]) can open the route for the use of ammonia in existing equipment. In this context, it is important to recall [6], that a given additive must match the requirements for both burning velocity and ignition behavior. Thus, the enhancement of burning velocity for use in spark-ignited engines must maintain high knock resistance, while for compression-ignition engines the ease of ignition of the fuel must be maintained as well. In addition, the development of new combustion technologies, such as reactivity-controlled compression ignition (RCCI), in which a low-reactivity fuel is ignited by faster autoignition of a high-reactivity fuel [7], could also allow the use of ammonia as a primary fuel in current engines with only modest modifications. For example, Reiter and Kong [8,9] modified a diesel engine to introduce ammonia into the intake manifold and to inject diesel or biodiesel directly into the cylinder to act as a pilot fuel. A similar injection strategy has been adopted by Gross and Kong [10] and Ryu et al. [11], choosing dimethyl ether (DME) as the pilot fuel to ignite ammonia.

Studies of fundamental combustion properties can facilitate the development of new fuels and tailor engine modifications to fuel properties. Consequently, autoignition measurements of ammonia blends with combustion promoters at well-defined conditions are crucial for understanding knock resistance and compression-ignition behavior of these blends. Moreover, such measurements are indispensable for the evaluation of chemical mechanisms describing ammonia oxidation, which can be used in models to simulate ignition behavior. Measurements and computations of the ignition behavior of NH_3 [12,13] and mixtures of NH_3 with H_2 [5,14,15] or CH_4 [6] have been reported. Mathieu and Petersen [12] reported shock tube measurements of ignition delay times of highly diluted NH_3/O_2 mixtures over a wide range of conditions, temperature (T = 1560 -2455 K), pressure (P) in the range 1.4 - 30 atm and equivalence ratio (φ) between 0.5 and 2.0, and presented a mechanism that predicted their measurements well. Shu et al. [13] measured the ignition delay of ammonia/air mixtures in a shock tube at

T = 1100 - 1600 K, P of 20 and 40 bar, and φ between 0.5 and 2.0. Their simulations using the mechanism of Mathieu and Petersen [12] also showed good agreement with their measurements. Pochet et al. [14] measured the ignition delay times of NH_3/H_2 mixtures (0, 10 and 25%vol. H_2) under fuel-lean conditions (φ = 0.2, 0.35, 0.5), high pressures (43 and 65 bar) and intermediate temperatures in the range 1000 - 1100 K in a rapid compression machine (RCM). Those authors evaluated the performance of five ammonia mechanisms from the literature (Konnov and De Ruyck [16], Zhang et al. [17], Song et al. [18], Dagaut and Nicolle [19], Nakamura et al. [20]) and found that none of the mechanisms predicted their measurements well. He et al. [15] reported RCM measurements of ignition delay time of NH_3 and NH_3/H_2 mixtures (1- 20% vol. H_2) at pressures from 20 to 60 bar, temperatures from 950 to 1150 K, and equivalence ratios from 0.5 to 2. They showed that, for their experimental conditions, the mechanism of Glarborg et al. [21] predicted pure NH_3 ignition delay times satisfactorily, but underpredicted the ignition delay times of the NH_3/H_2 mixtures by a factor of 3 (at P = 20 and 40 bar), while the mechanism from Klippenstein et al. [22] gave improved performance for the NH_3/H_2 mixtures, but overpredicted the results for pure NH_3 by more than a factor of 5. Recently, Dai et al. presented measurements of ignition delay time of NH_3 and NH_3/H_2 mixtures [5], and NH_3/CH_4 mixtures [6], in an RCM. Pure NH_3 was studied for the ranges T = 1040 - 1210 K, P = 20 - 75 bar and φ = 0.5 - 3.0, while NH_3/H_2 mixtures with H_2 fractions from 0 to 10% were studied at equivalence ratios of 0.5 and 1.0. In that paper, a modified mechanism based on that from Glarborg et al. [21], with an updated rate constant for the reaction $NH_2+NH_2(+M)=N_2H_4(+M)$, was proposed. Simulations using this mechanism [5,21], and mechanisms from Mathieu and Petersen [12], Klippenstein et al. [22] and Shrestha et al. [23], were compared with the measurements in [5]. In general, the updated mechanism of Glarborg et al. [5,21] gave the best predictions: for pure NH_3 and NH_3/H_2 mixture at high pressures (40–60 bar) they were generally within 40% of the experimental results, but underpredicted the ignition delay times at lower pressures, consistent with the observations of He et al. [15]. The NH_3/CH_4 mixtures, with CH_4 fractions of 0, 5, 10 and 50% were studied at equivalence ratio φ = 0.5, pressures from 20 - 70 bar and temperatures from 930 to 1140 K [6]. In addition, measurements were performed for NH_3 mixtures with 10% CH_4 at φ = 1.0 and 2.0. The ability of mechanisms from Glarborg et al. [5,21], Shrestha et al. [23], "San Diego" [24], Tian et al. [25], "Li-Konnov" [26] and Okafor et al. [27] to predict the ignition results were evaluated; here too, simulations using the updated mechanism of Glarborg et al. [5,21] showed the best agreements with measurements, with differences being generally less than 30% for all

the conditions investigated. Very recently, Yu et al. [28], using n-heptane as a diesel surrogate, measured ignition delay times of NH_3/n-heptane mixtures in an RCM in the range T = 635–945 K, at pressures of 10 and 15 bar, and equivalence ratios of 1.0 and 2.0 with 0%, 20%, and 40% of the fuel energy contributed by NH_3. An NH_3/n-heptane mechanism was assembled based on the n-heptane mechanism from Zhang et al. [29] and the (original) NH_3 mechanism from Glarborg et al. [21]; significant discrepancies between experiments and the simulations were observed.

For the purposes of making ammonia suitable for compression-ignition engines, DME is an attractive candidate, having similar autoignition properties to diesel [30] with a substantially lower tendency to form soot. While the autoignition properties of DME have been studied in detail [31–34], to our knowledge, no reports of the ignition delay times of NH_3/DME mixtures are publicly available. In the framework of an ignition-enhancing "additive", the preferred composition contains the lowest fraction of the additive that maintains efficacy. Investigation of low DME fractions is further motivated by the non-linear ignition-promoting effect of DME observed in studies of DME/methanol [35] and DME/n-butane [36] mixtures. From a practical perspective, it is also important to extend the range of measurements to conditions closer to the operating point of modern (turbocharged/supercharged) diesel engines. In this paper, we report the ignition delay times of NH_3/DME mixtures measured in an RCM at equivalence ratios of 0.5, 1.0 and 2.0, with DME fractions in the fuel of 0, 2%, 5% and 100%, pressures in the range 10 - 70 bar and temperatures from 620 K to 1140 K. In addition, a new NH_3/DME mechanism is presented that is based on previous studies [5,21,37], drawing also on recent results by Stagni et al. [38]. The mechanism includes a novel subset describing NH_3/DME interactions, for which the key reaction $NH_2+CH_3OCH_3 = NH_3+CH_3OCH_2$ is studied by ab initio methods. The performance of the model is compared with the experimental results. A kinetic analysis based on this mechanism is performed to gain more insight in the ignition process of NH_3/DME mixtures under the conditions studied.

2. Experiments and simulations

2.1. Experimental setup

The RCM used to measure the ignition delay times has been described elsewhere [39,40], and only a brief description will be given here. The gas mixtures were compressed in ~ 10-20 ms to peak pressure, with 80% of the compression occurring in less than 3 ms. The pressure trace was measured by a Kistler ThermoComp quartz pressure sensor with thermal-shock-optimized

construction. A creviced piston head is used in this machine to obtain a homogenous reacting core during the experiment [41]. The temperature after compression (T_c) was obtained assuming the existence of an adiabatic core, using the standard thermodynamic formulation for adiabatic compression (see [39,40], for example); the temperature-dependent heat capacities of the reactants are taken from [21,37]. Since the RCM used in this study does not have a means to vary the initial temperature reliably, the compression temperature T_c can only be varied by changing the compression ratio and/or changing the heat capacity of the mixture. The maximum compression ratio is 22.5, which limits the temperature that can be obtained at constant composition. Consequently, to obtain similar temperatures after compression, different gas mixtures have been diluted by different ratios of N_2 and Ar while keeping the total fraction (N_2+Ar) constant. For measurements of pure DME, CO_2 is used instead of Ar. When the initial temperature, compression ratio and composition are fixed, the compression pressure P_c can be varied by changing the initial pressure P_0 to perform measurements along isotherms. The compositions (in mole fraction) of the mixtures examined in detail here are shown in Table 1. Results for other inert compositions, in which the temperature is varied at lower pressures, are included in the Supplementary Material.

Table 1. Compositions of NH_3/DME mixtures studied in this work (unit: mole fraction)

Mixtures	φ	DME/fuel	NH_3	DME	O_2	N_2	Ar	CO_2
Mixture 1*	0.5	0	0.1	0	0.15	0.1	0.65	0
Mixture 2	0.5	2%	0.095	0.002	0.153	0.4	0.35	0
Mixture 3	0.5	5%	0.087	0.005	0.158	0.5	0.25	0
Mixture 4	0.5	100%	0	0.036	0.214	0.45	0	0.3
Mixture 5*	1.0	0	0.143	0	0.107	0	0.75	0
Mixture 6	1.0	2%	0.136	0.003	0.111	0.4	0.35	0
Mixture 7	1.0	5%	0.128	0.007	0.116	0.5	0.25	0
Mixture 8	1.0	100%	0	0.063	0.188	0.45	0	0.3
Mixture 9*	2.0	0	0.182	0	0.068	0	0.75	0
Mixture 10	2.0	2%	0.175	0.004	0.071	0.15	0.6	0
Mixture 11	2.0	5%	0.166	0.009	0.075	0.55	0.2	0
Mixture 12	2.0	100%	0	0.1	0.15	0.65	0	0.1

* Compositions and data taken from [5].

All gas mixtures were prepared in advance in a 10-L gas bottle, used to charge the combustion chamber to the required initial pressure. The mixtures were allowed to mix for

least 24 hours to ensure homogeneity. As done in our previous studies [5,6], to remove any effect of the adsorption of ammonia on the metal surfaces of the facility on the ignition delay time measurements, passivation of the surfaces was done following the procedure proposed by Mathieu and Petersen [12]: the mixing tank and RCM were filled with pure ammonia (10 mbar) for roughly 10 min and then evacuated to 0.7 mbar.

For single-stage ignition, the ignition delay time is taken from the end of compression to the point a maximum slope during ignition. Two-stage ignition was observed in some of the NH_3/DME mixtures studied. In these cases, the ignition delay time of the first stage (τ_1) was defined as the interval between the end of compression and the maximum pressure rise in the first stage, while the overall ignition delay time (τ) is defined as the interval between the end of compression and the maximum of pressure rise in the second stage. These times are illustrated in Fig. 1. The day-to-day reproducibility of the measurements, including repositioning of the piston height, was determined to be better than 5%. The uncertainty of the calculated core gas temperature (T_c) is less than ± 3.5 K for all measurements [42].

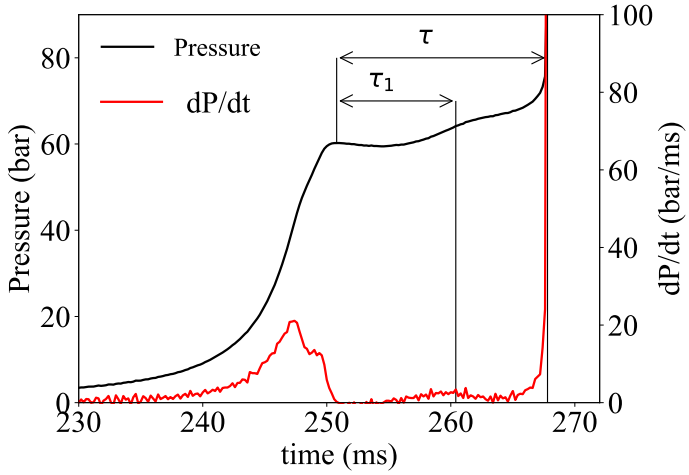

Figure 1. Measured pressure (black line) and rate of change of the pressure (red line) of Mixture 7 at T_c = 950 K, P_c = 60 bar. The vertical black lines show the maximum in the derivative of the pressure, indicating the points at which the ignition delay times were taken.

2.2. Numerical approach

2.2.1 Chemical kinetic model

The chemical kinetic model was an updated version of the mechanism proposed in the review of Glarborg et al. [21]. This mechanism was, with minor changes, used successfully in our previous studies of ignition delay of NH_3, NH_3/H_2 and NH_3/CH_4 mixtures [5,6]. In the present work, the amine subset was updated and the model was extended with subsets for DME, drawn from the high pressure study of Hashemi et al. [37], and for DME/NH_3 interactions. The

complete kinetic model, including thermodynamic properties, is available in Supplementary Material.

The amine subset of the model was updated, based on the recent work of Stagni et al. [38]. They studied a number of key reactions in the NH_3 mechanism by ab initio methods and established a kinetic model, whose performance they verified over a wide range of conditions. We have adopted their theoretical rate constants for the reactions $NH_3(+M) = NH_2+H(+M)$, $NH_3+HO_2 = NH_2+H_2O_2$, $NH_3+O_2 = NH_2+HO_2$, and $HNO(+M) = H+NO(+M)$. By far the most important of these changes concerns NH_3+O_2, which proceeds rapidly in the reverse direction, i.e., $NH_2+HO_2 = NH_3+O_2$. Without this very fast chain-terminating step, it was not possible to predict satisfactorily the observed ignition delay times for the DME/NH_3 mixtures. However, the rate constant calculated by Stagni et al. [38] for NH_2+HO_2 is much faster at room temperature than reported experimental data [43,44] and more work on this step is desirable. Also, the importance of other product channels for NH_2+HO_2, i.e., $HNO+H_2O$ and H_2NO+OH, is in discussion. Following Stagni et al. [38], rate constants in the HONO/HNO_2 subset were drawn from the recent theoretical work of Goldsmith and coworkers [45] and a few rate constants for H_2NO reactions were modified.

The mechanism of Hashemi et al. [37] did not provide a good description of ignition delays for DME measured in shock tubes and RCMs. In the present work, a few modifications were made to improve its performance. The rate coefficients for thermal dissociation of CH_3OCH_2 to form $CH_2O + CH_3$ was drawn from the recent theoretical study by Gao et al. [46], while for the dissociation of HO_2CH_2OCHO to $OCH_2OCHO + OH$, we multiplied the rate constant by a factor of two compared to the estimate of Burke et al. [32].

There are no kinetic studies of DME/NH_3 interactions reported in the literature and a reaction subset was established as part of the present work. Table 2 shows selected reactions in the DME/NH_3 subset. Several classes of reactions are relevant for this interaction. The NH_2 radical may abstract H-atoms from the DME and from stable intermediates formed in DME oxidation. The most important step is the NH_2 + DME reaction,

$$CH_3OCH_3+NH_2=CH_3OCH_2+NH_3 \qquad (R1)$$

There are no experimental data available for the rate constant of R1. As part of the present work, we calculated the rate constant from ab initio theory. Reactants and transition states were examined computationally with the Gaussian 16 program [47]. Density functional theory (M06-2X/6-311+G(2df,2p) [48] was used to obtain geometries and vibrational frequencies. The latter were scaled by recommended factors of 0.971 for zero-point energy and by 0.946

for fundamental frequencies [49]. Low-frequency torsional modes were treated as separable hindered rotors with sinusoidal potentials. Next, single-point energies were computed with the CBS-APNO methodology, which approximates an infinite-basis coupled-cluster calculation [50]. Thermochemical and transition state theory parameters were calculated via the Multiwell program [51]. The calculated value, $k_1 = 4.5\ T^{3.61}\ \exp(-1184/T)$, is in reasonable agreement with the rate constant reported for $C_2H_6 + NH_2$ [52]. However, using this rate constant in the model led to predictions of ignition delays for the DME/NH_3 mixtures that were much shorter than observed. To improve the agreement with experiment, we adopted a lower limit value for k_1; reducing the A-factor by 2.5 and increasing the activation energy by 2 kcal/mol. It should be noted that we believe that the ab initio rate constant for $CH_3OCH_3+NH_2$ is fairly accurate and consider the revised value of k_1 to be an "engineering modification" that compensates for other short-comings in the mechanism, possibly in the amine subset.

Table 2. Selected reactions in the DME/NH_3 subset of the reaction mechanism. Rate constants are listed in the form $A*T^N*\exp(-E_a/RT)$. Units are calories, cm^3, mol, second.

	Reaction Mechanism	A	N	E_a	Source
1.	$CH_3OCH_3+NH_2=CH_3OCH_2+NH_3$	1.8E00	3.610	4353	pw, lower limit[a]
2.	$CH_3OCH_3+NO_2=CH_3OCH_2+HONO$	5.8E01	3.500	23755	Guan et al. [53]
3.	$CH_3OCH_3+NO_2=CH_3OCH_2+HNO_2$	6.5E02	3.000	23176	Guan et al. [53]
4.	$CH_3OCH_2+NH_2(+M)=CH_3OCH_2NH_2(+M)$	7.2E12	0.420	0	$k_{CH3+NH2}$
	Low pressure limit	2.2E30	-3.850	0	
5.	$CH_3OCH_2+NO_2=CH_3OCH_2O+NO$	1.1E13	0.000	0	$k_{CH3+NO2}$
6.	$CH_3OCH_2OO+NH_3=CH_3OCH_2OOH+NH_2$	3.0E11	0.000	22000	$k_{NH3+HO2}$
7.	$CH_3OCH_2OO+NH_2=CH_3OCH_2O+H_2NO$	3.0E13	0.000	0	est
8.	$CH_3OCH_2OO+NO=CH_3OCH_2O+NO_2$	1.4E12	0.000	-715	est $k_{CH3OO+NO}$
9.	$O_2CH_2OCH_2O_2H+NO=OCH_2OCH_2O_2H+NO_2$	1.4E12	0.000	-715	est $k_{CH3OO+NO}$

a: From ab initio calculations, $k_1 = 4.5\ T^{3.61}\ \exp(-1184/T)$.

As described in section 2.1, two-stage ignition was observed for DME+NH_3 mixtures. In the period leading to first-stage ignition, a minor fraction of the ammonia is oxidized to NO_x and reactions of DME with nitrogen oxides maybe important for the multi-stage behavior observed. DME/NO_x interactions were studied in detail recently by Shrestha et al. [54]. A comprehensive kinetic model was presented for dimethyl ether and dimethoxymethane oxidation, including NO_x interaction, utilizing experimental laminar flame speed

measurements at elevated pressure and temperature. While DME+NO is too slow to be of importance, the reaction with NO_2 is sufficiently fast to play a role,

$$CH_3OCH_3+NO_2=CH_3OCH_2+HONO \qquad (R2)$$

$$CH_3OCH_3+NO_2=CH_3OCH_2+HNO_2 \qquad (R3)$$

The rate constants for R2 and R3 were adopted from the recent theoretical study by Guan et al. [53]. Other reactions between NH_2 and stable species include $CH_4 + NH_2$, already included in the starting mechanism [21], and $CH_2O + NH_2$, drawn from the theoretical study by Li and Lu [55]. The NH_2 radical may also recombine with radicals formed in DME oxidation, primarily

$$CH_3OCH_2+NH_2(+M)=CH_3OCH_2NH_2(+M) \qquad (R4)$$

and $CH_3+NH_2(+M)=CH_3NH_2(+M)$ (which was also part of the mechanism in [21]). The $CH_3OCH_2+NH_2(+M)$ reaction was included with a rate constant similar to $CH_3+NH_2(+M)$. As part of the present work, thermodynamic properties for the $CH_3OCH_2NH_2$ adduct (1-methoxy-methanimine) and the derived radicals were calculated from ab initio methods. The enthalpy of formation of $CH_3OCH_2NH_2$ was derived via the isodesmic reaction $CH_3OCH_2NH_2 + CH_4 = CH_3OCH_3 + CH_3NH_2$ and the radicals via the C-H or N-H bond strength and the heats of formation of H and $CH_3OCH_2NH_2$. These computed bond strengths at 298 K are H--$CH_2OCH_2NH_2$ = 97.04 kcal/mol, CH_3OCH(--H)NH_2 = 93.84 kcal/mol, and CH_3OCH_2NH--H 101.1 kcal/mol. A reaction subset for this component was included in the mechanism. However, the thermal stability of $CH_3OCH_2NH_2$ was too low for this pathway to be important under the conditions investigated.

The $CH_3+NH_2(+M)$ reaction forming methylamine had a larger impact on modeling predictions. For this step we adopted the rate coefficients from Jodkowski et al. [56]; they offer a better extrapolation to high pressure than the shock tube measurements of the reverse step by Votsmeier et al. [57]. The CH_3NH_2 subset was drawn from the recent work of Glarborg et al. [58]. At high pressure and not too high temperature (500–900 K), CH_3OCH_2OO is formed from recombination of CH_3OCH_2 and O_2 [31]. Internal H-abstraction and subsequent O_2 addition could yield another peroxide, $O_2CH_2OCH_2O_2H$. These peroxides may abstract a hydrogen atom from NH_3, but from analogy with $NH_3 + HO_2$, these steps would be expected to be slow. However, the peroxides would react rapidly with nitric oxide formed from the oxidation of NH_3,

$$CH_3OCH_2OO+NO=CH_3OCH_2O+NO_2 \qquad (R8)$$

$$O_2CH_2OCH_2O_2H+NO=OCH_2OCH_2O_2H+NO_2 \qquad (R9)$$

For both reactions, we have estimated the rate constant by analogy to CH_3OO+NO. The $OCH_2OCH_2O_2H$ adduct is expected to dissociate rapidly; we have tentatively assumed formation of $2CH_2O+HO_2$.

2.2.2 Simulation methods

The ignition process of the mixtures measured in the RCM was simulated using the homogenous reactor code from the Cantera package [59]. The default absolute tolerance 1e-15 was used in the simulations; increasing the tolerance to 1e-20 changed the computed delay times by less than 0.5%. To account for changes in the mixture conditions during compression (including possible heat release) and post-compression heat loss, the specific volume of the adiabatic core was used as input in the simulations. The specific volume was derived from the measured pressure trace of a non-reactive gas mixture that had the same average heat capacity as the reactive mixture [5,60]. We note that significant pre-ignition heat release was observed for several of the experimental conditions studied, arising either from two-stage ignition or from a process reminiscent of that observed for t-butanol ignition by Weber and Sung [61]. While the use of the specific volume from the non-reactive pressure trace in this case can result in computed overall ignition delay times that tend to be too short, the magnitude of the resulting discrepancy has been estimated to be less than 30% [62]. As done in other systems showing pre-ignition heat release (for example, [31,32,35,36,62]), we follow the same approach here, while cognizant of its shortcomings. For the kinetic analysis, simulations at constant specific volume were performed to avoid the complications in interpretation caused by post-compression heat loss.

Sensitivity analyses were performed to identify the most important reactions controlling the autoignition behavior. The sensitivity coefficient (S_i) for a specific reaction is obtained from:

$$S_i = \left(\frac{\Delta\tau}{\tau}\right) / \left(\frac{\Delta k_i}{k_i}\right), \quad (2)$$

where $\Delta\tau$ is change of ignition delay time corresponding to change of rate constant Δk_i of *i*th reaction. In this study, each rate constant is increased by factor of 2 by doubling the pre-exponential A factor while keeping those of the other reactions constant. A negative S_i indicates an ignition-promoting effect (decreasing the ignition delay time when a rate constant is increased) and a positive coefficient denotes ignition inhibition (increasing ignition delay time with increasing rate constant). An element flux analysis was performed to study the

reaction path of the fuels under the experimental conditions. Rate-of-Production (ROP) analyses were also performed to assist the interpretation of the results. For convenience, these analyses maintained a fixed inert composition (75% N_2).

3. Results and discussion

3.1 Characteristics of the ignition profile

Three different kinds of ignition behavior were observed in the experiments; examples are shown in Fig. 2. "Normal" single-stage ignition (steep pressure increase after the post-compression period) was observed in all pure NH_3 measurements and in part of the measurements on pure DME at high pressures. Two-stage ignition phenomena were observed in some of the pure DME measurements at low pressures and in NH_3/DME blends at φ =1.0 and 2.0. Further, as mentioned above, a pre-ignition pressure rise, a slow rise in pressure over several milliseconds prior to ignition, was reproducibly observed in NH_3/DME blends at φ = 0.5. This phenomenon has been reported previously in the NH_3/CH_4 study by Dai et al. [6], where the pressure rise was observed at 50% CH_4 with high reproducibility, as observed in [61], in contrast to reports for NH_3 [17] and ethanol [63], reporting only irregular occurrence.

The simulated pressure profiles of NH_3 with 2% DME at φ = 0.5 and with 5% DME at φ = 1.0 are shown in Fig. 3. At φ = 0.5 (Fig. 3a), while the computed time of ignition is 18% longer than the measurement, the simulated pressure follows the experimental slow pre-ignition pressure rise faithfully. We note that the mechanism used in [6] failed to predict this phenomenon for ammonia/methane mixtures. At φ = 1.0 (Fig. 3b), the simulated pressure profile also shows two-stage ignition, but with the simulated first-stage ignition being closer to the second-stage ignition than shown in the experiment; as a result, the computed two-stage ignition resembles the slow pre-ignition pressure rise seen in Fig. 3a. We also note that, for 5% DME in the fuel at φ = 0.5, both the experiments and simulations show a "shoulder" superimposed on the pre-ignition pressure rise, close to the time taken for overall ignition, suggesting two-stage ignition. While this shoulder in the simulation is just clear enough to extract a first-stage ignition delay time, we only report its existence here, and compare the overall delay times for these conditions. Also noteworthy is the observation that, for some of the experiments, more often those having an overall ignition delay time of roughly 10 ms or lower, a slightly higher P_c (generally less than 2 bar) was observed in the reactive mixtures than measured in the non-reactive mixture. This observation indicates that DME generates some heat release during compression, even for relatively long ignition delay times. We discuss

the role of these phenomena in the effect of DME on ammonia ignition in Sec. 3.5.1, below. We report in passing that simulations using the mechanism from Shrestha et al. [54] did not exhibit two-stage ignition in experiments in which it was observed and for some experimental conditions failed to show any ignition. Consequently, we do not consider this mechanism further, but include the results in the Supplementary Material.

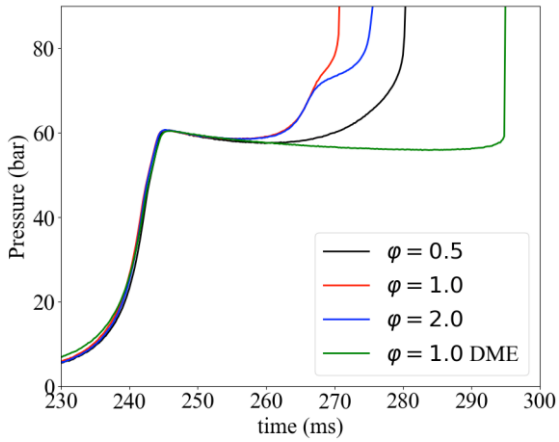

Figure 2. Measured pressure traces of NH_3 with 2% DME at T_c = 950 K and P_c = 60 bar. Two-stage ignition is shown at φ= 1.0 and 2.0, slow, pre-ignition pressure rise at φ= 0.5. The curve for DME at φ= 1.0 and 625 K represents "normal" ignition.

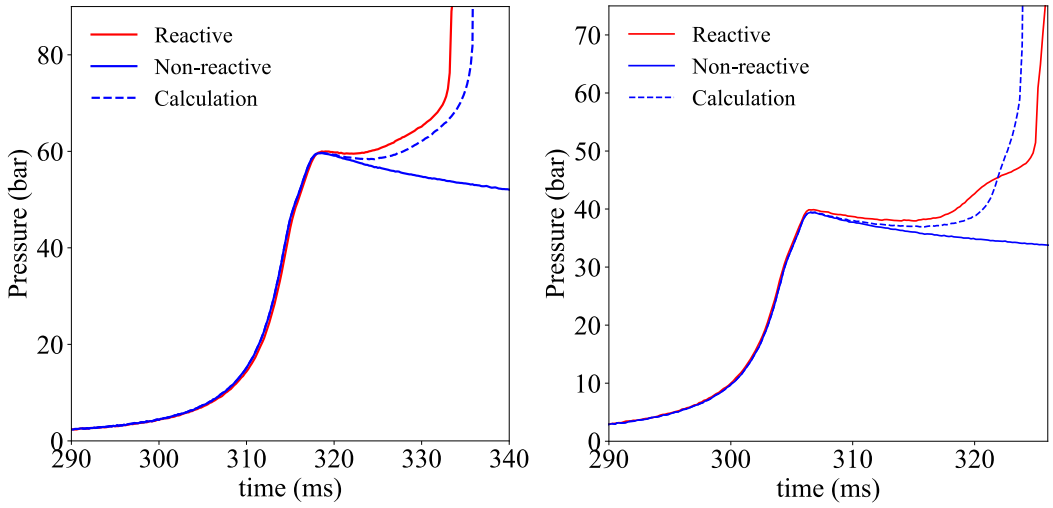

(a) (b)

Figure 3. Measured (solid red line = reactive mixture, solid blue line = non-reactive mixture) and calculated (dashed blue line) pressure traces of the ignition process of NH_3 with 2% DME at φ = 0.5, P_c = 60 bar, T_c = 965 K (a) and NH_3 with 5% DME at φ= 1.0 P_c= 40bar, T_c = 900 K (b).

Referring to the simulated result in Fig. 3b, we note that using the original rate constant for reaction R1, obtained from the ab initio calculations discussed above, significantly

advances the first stage of ignition and results in a more discernable first stage more resembling the experimental trace. However, use of this rate constant also substantially shortened the overall ignition delay time and showed substantial heat release during compression for all experimental conditions, at variance with the experimental results. Consequently, we use the rate expression in its current form (Table 2) below, which also reproduces the slight increase in P_c for some of the DME experiments noted above well. Subsequent research will examine the mechanism to allow better replication of the two-stage ignition shown in the experiments. We further note that post-compression heat loss tends to exaggerate differences between mechanisms: depending on the ignition delay, and thus on the change in temperature during the simulation, changes in mechanism that result in "modest" changes in ignition delay time (~50%) when computed at constant volume can become a factor of 5 when using the experimental pressure trace. Heat loss also tends to reduce the prominence of the first stage when compared to constant-volume simulations; in these cases, the "shoulder" in the ignition curves mentioned for φ = 0.5 and 5% DME above is seen as two-stage ignition in simulations at constant volume.

Regarding the pre-ignition heat release, assuming that the change in pressure occurs adiabatically, we estimate the concomitant increase in temperature from the experimental pressure traces to be roughly 50 K above the initial T_c. Of course, there is also heat loss from the adiabatic core during this period that should be considered in the estimate. For this purpose, we compare the reacting temperature with what would be expected in the absence of heat release, i.e. in the adiabatic core derived from the non-reactive pressure trace (with the caveat described above). The temperature difference between reactive and non-reactive case is roughly 100 K. We note that the estimated increase in temperature is roughly the same for both slow pre-ignition pressure rise and from first-stage ignition. As will be discussed in Sec. 3.5.3, we consider the pre-ignition heat release as an important part of the ignition process for DME/NH_3 mixtures.

3.2 Effect of DME fraction

To explore the sensitivity of ammonia ignition to variation in the DME fraction at these low levels, experiments were performed for NH_3/DME mixtures at P_c = 60 bar with DME fractions of 2% (Mixtures 2, 6 and 10 in Table 1) and 5% (Mixtures 3, 7 and 11); the results are shown in Fig. 4. For the purposes of comparison, results are also presented for pure ammonia (Mixtures 1, 5 and 9, data taken from [5]) and pure DME (Mixtures 4, 8 and 12, measured here). The variations with temperature at other pressures are given in the

Supplementary Material. Both the overall and first-stage ignition delay times decrease monotonically with increasing temperature for all mixtures and conditions. Thus, despite the observation of two-stage ignition, the results do not show evidence of a negative-temperature-coefficient (NTC) region for the range of temperatures studied. DME shows a substantial ignition-enhancing effect on ammonia. For example, at φ = 0.5 (Fig. 4a), 2% DME in the mixture reduces the compression temperature T_c at which the overall ignition delay time is ~40 ms from ~1080 K for pure ammonia to ~930 K. Increasing the DME fraction to 5% reduces T_c further to ~830 K, while the pure DME mixtures studied have an ignition delay time of 40 ms at ~ 630 K. These results also indicate the non-linear effect of DME on ignition delay, i.e., that the ignition-enhancing effect of DME decreases at higher DME fraction, which was observed in studies of DME/methanol [35] and DME/n-butane [36]. For comparison, in DME/methanol mixtures [35], roughly 40% DME was needed to effect a reduction in T_c of 150 K to maintain a given ignition delay time, compared with 2% DME in ammonia. Strong reduction in reaction temperature and the flow-reactor equivalent of two-stage ignition was also reported for small DME fractions in methane at high pressure [37].

Anticipating the analysis in Section 3.5.2, below, we compare the reduction in T_c necessary to maintain a constant ignition delay time observed here with those reported for admixture of other fuels with ammonia [5,6]. At φ = 0.5 and 60 bar, a fraction of 10% hydrogen in the fuel [5] decreased T_c by ~100 K and 50% methane [6] resulted in a decrease of ~125 K, while 5% DME under the same conditions decreases T_c by ~250 K. Thus, admixture of small fractions of DME enables ignition at temperatures far outside the normal envelope for pure ammonia.

The large shifts in the curves of ignition delay time with temperature make it difficult to compare the changes in ignition delay caused by DME addition directly. Referring to Fig. 4a, we observe that the overall ignition delay time of the NH_3/DME mixtures is reduced by roughly one order of magnitude when increasing DME fraction from 2% to 5% at φ = 0.5 and T_c= 900 K. A similar effect of DME addition is observed at φ = 1.0 and 2.0. The first-stage ignition delay times are also reduced by an order of magnitude when increasing the DME fraction from 2% to 5% for mixtures at φ = 1.0 and 2.0 as shown in Figs. 4b and c. The interval between the first stage ignition and overall ignition is more pronounced at higher φ and lower DME fraction. By analogy with other fuels and fuel mixtures (for example, in [34,36,39,40]), the shortening of the first-stage relative to the overall delay time with increasing temperature observed in Fig. 4b,c for 2% DME suggests that something resembling an NTC region exists at higher temperatures than those measured here. Since the ignition delay times under these conditions

approach 1 ms, shock-tube measurements are indicated to consider this behavior in more detail, as done in [32]. That 2% DME in ammonia (<0.5% DME in the combustible mixture, see Table 1) results in two-stage ignition, while ammonia itself does not show complex ignition behavior, is in our opinion noteworthy and certainly the strong effect for which one hopes when considering the use of an ignition-enhancing "additive".

As shown in Fig. 4, the calculated ignition delay times using the mechanism from this study are in good agreement with the measurements for both pure NH_3 and pure DME, with a maximum deviation less than 30% for all conditions except that for pure ammonia at φ = 2.0, where overprediction up to a factor of ~ 6 is observed at the lowest temperature. We note here that for pure ammonia the revised ammonia submechanism predicts the ignition delay time as well as that in [5] at φ = 0.5 and 1.0, but with a significant loss of performance φ = 2.0. For NH_3/DME mixtures, the mechanism reproduces the trends in the ignition delay times with T_c for the NH_3/DME mixtures at all equivalence ratios. At φ = 0.5, the computations generally agree with the measured overall ignition delay times to 50% or better for both 2% and 5% DME. As illustrated in Fig. 3a, the computations for 2% DME shows only a pre-ignition pressure rise at this equivalence ratio, in accordance with the measurements, and show "shoulders" in the ignition curves at 5% DME, as reported above, in general agreement with the experiments. At φ =1.0, the mechanism also predicts the overall ignition delay times well for both 2% and 5% DME, with a maximum deviation ~75% at 1025 K. The calculations show resolved two-stage ignition at 800-850 K for 5% DME; the differences between the simulated and measured first-stage delay times are less than 50% in that temperature range. At φ =1.0, the computations for 2% DME show only the slow pressure rise, in contrast to the two-stage ignition observed in the experiments. At φ = 2.0, the mechanism again predicts the overall ignition delay times generally to within 50% for both DME fractions, with the exception of 5% DME at ~775 K, where the overall ignition delay time is overpredicted by a factor of 2.5. At this equivalence ratio, the calculations predict resolved two-stage ignition for 2% DME in the fuel, although the first-stage ignition delay times are overpredicted by a factor of ~2.5 at 920-975 K. At higher temperatures, the calculated pressure curves show pre-ignition pressure rise instead of a resolved two-stage ignition. For 5% DME, the calculated first-stage delay times agree with those measured by better than 50%, except at 775 K where the predicted delay time is a factor of 3 too high.

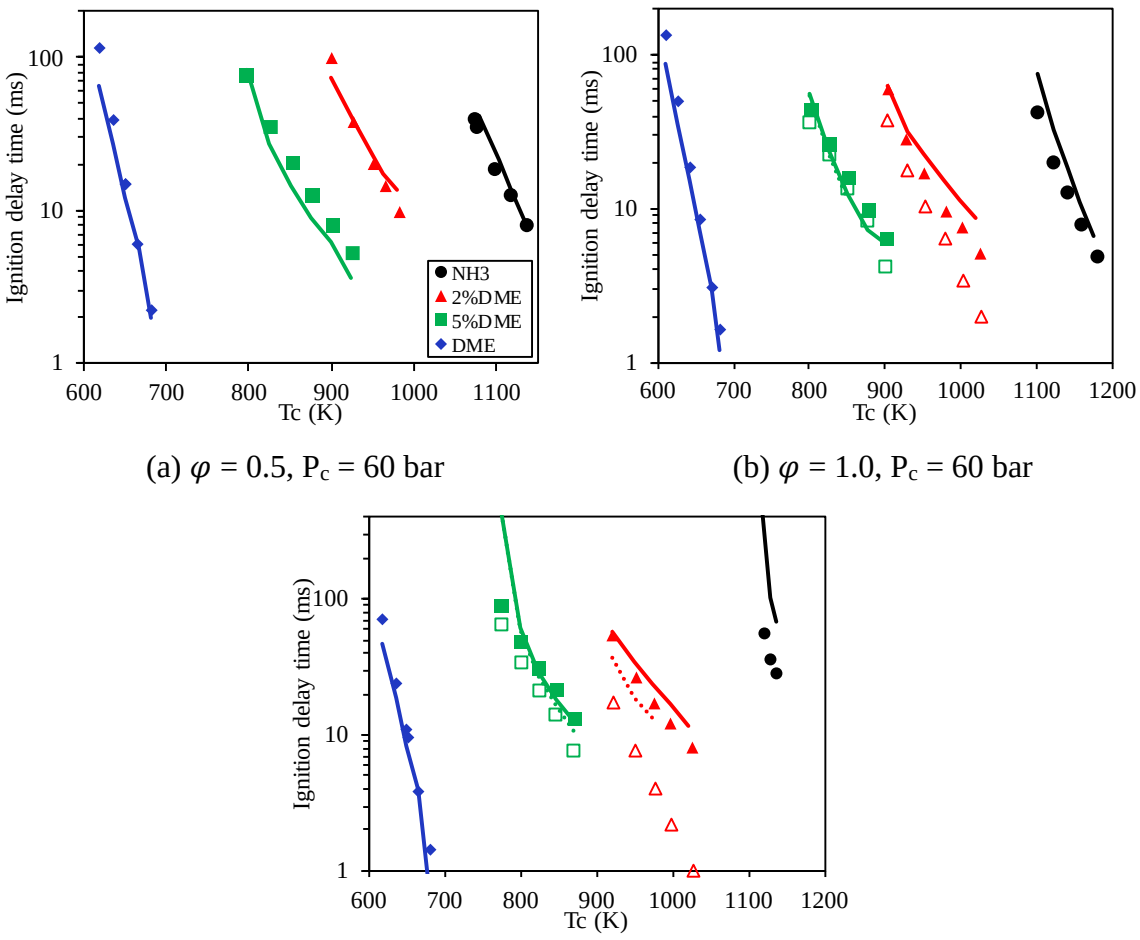

(a) φ = 0.5, P_c = 60 bar

(b) φ = 1.0, P_c = 60 bar

(c) φ = 2.0, P_c=60 bar

Figure 4. Measured and calculated ignition delay times of NH_3 with different DME fraction in the fuel mixtures. τ (closed symbols) and τ_1 (open symbols). Note: the error bars of ignition delay times ($\pm$5%) are covered by the symbols and thus not visible in the figures.

3.3 Effect of equivalence ratio

The measured ignition delay times from Fig. 4 are rearranged to expose the effect of equivalence ratio. As discussed in [5] and shown in Fig. 5a, the ignition delay time of pure NH_3 increases with equivalence ratio, by a factor of 2 when φ increases from 0.5 to 1.0 and by another factor of 2 when going from 1.0 to 2.0. At 2% DME in NH_3, Fig. 5b, the variation with equivalence ratio has been drastically reduced: the ignition delay times at φ = 0.5 and 1.0 now agree within the experimental uncertainty (less than 5%) at T_c higher than 930 K, while increasing φ from 1.0 to 2.0 increases the ignition delay times by ~50%. Increasing the fraction of DME from 2% to 5%, as seen in Fig. 5c, all but erases the variation with equivalence ratio, with the maximum differences being ~30% (φ = 1.0 as compared to at φ = 0.5 and 2.0). The lack of variation resembles the results for pure DME in Fig. 5d, which also show only a modest impact of equivalence ratio, with the ignition delay times at φ = 0.5 tending to be somewhat

longer (~50%). The trends for pure DME with equivalence ratio observed here at 60 bar are similar to those reported at lower pressures (10-30 bar) by Mittal et al. [34] and Burke et al. [32]

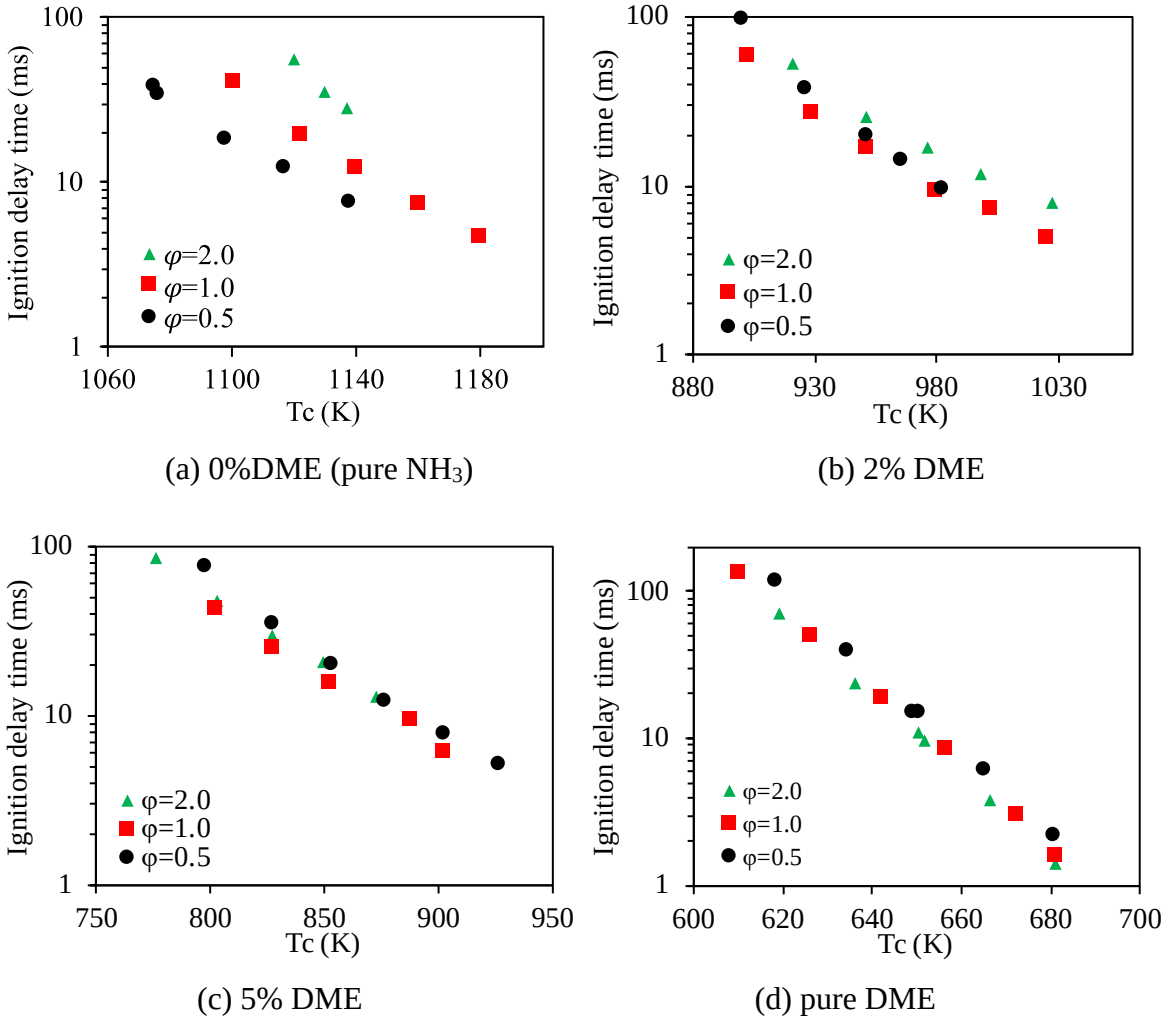

(a) 0%DME (pure NH_3) (b) 2% DME

(c) 5% DME (d) pure DME

Figure 5. Effect of equivalence ratio on the overall ignition delay times (τ) at three DME fractions at P_c = 60 bar, pure NH_3, taken from [5] (a), 2%DME (b), 5%DME (c) and pure DME (d). Circles - φ = 0.5, squares – φ = 1.0 and triangles – φ = 2.0.

3.4 Effect of pressure

The ignition delay times of NH_3/DME mixtures were measured as function of pressure at φ = 0.5, 1.0 and 2.0. The results at φ = 0.5 and T= 1140, 980, 900 and 680 K for pure NH_3, 2% DME, 5% DME and pure DME, respectively, are shown in Fig. 6; the results for φ = 1.0 and 2.0 are included in the Supplementary Material. Both first stage (at for φ = 1.0 and 2.0) and overall ignition delay times are reduced with increasing compression pressure (P_c). The present mechanism predicts the pressure dependence of the ignition delay times of pure NH_3 at φ = 0.5 and 1.0, with a maximum deviation less than 25%, but overpredicts the results up to a factor of

3 at φ = 2.0, as discussed above by Fig. 4c. For 2% DME in NH_3, the pre-ignition pressure rise is observed in the simulations at all pressures for at φ = 0.5, 1.0 and 2.0, with the calculated (overall) ignition delay times generally agreeing with the measurements to better than 50% at all three equivalence ratios. At 5% DME and φ = 0.5, the mechanism underpredicts the pressure dependence of the overall ignition delay times by roughly 50%, similar to that observed in the temperature dependent measurements shown in Fig. 4(a). As noted in Section 3.1, at φ = 0.5 and 5% DME, both the experiments and simulations show a shoulder in the ignition curve towards the end of the pre-ignition period; this is also observed at other pressures.

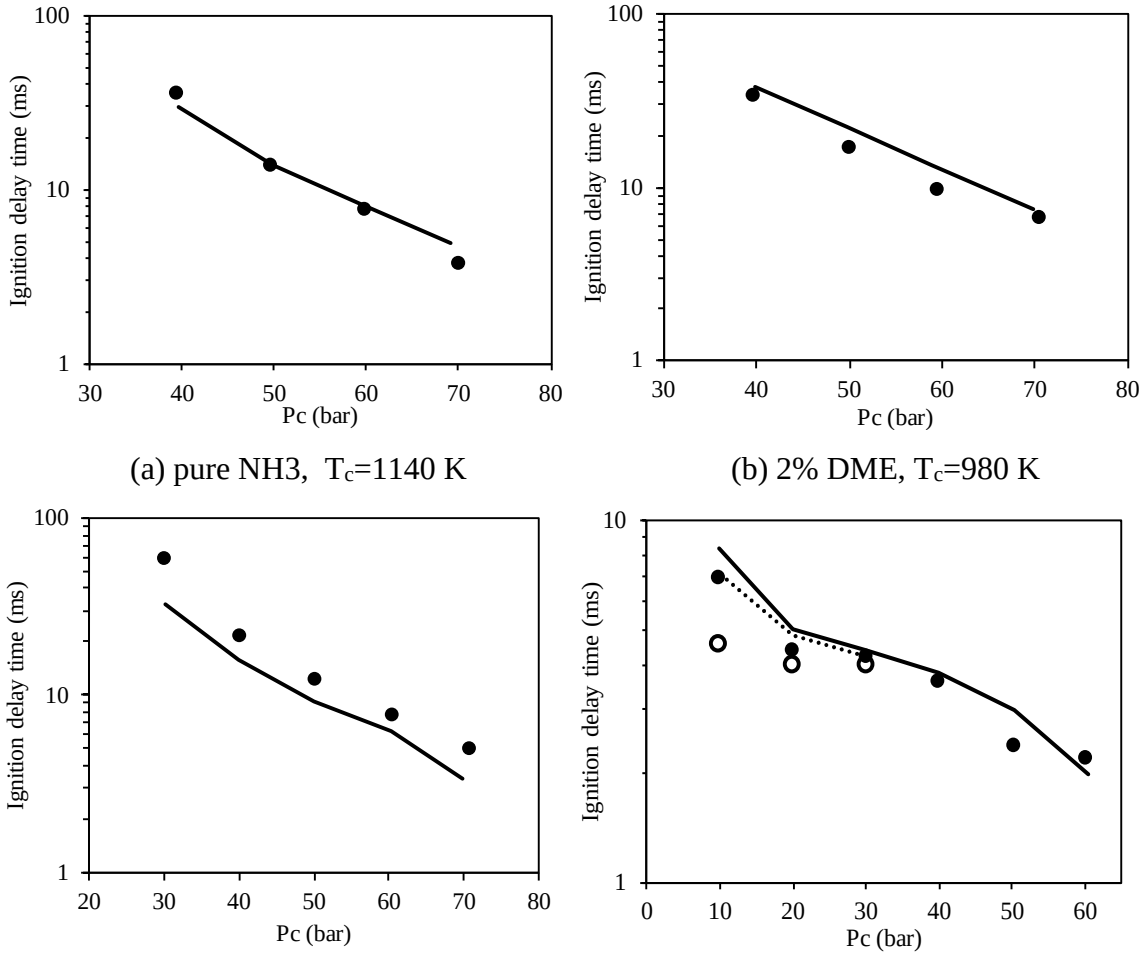

(a) pure NH3, T_c=1140 K

(b) 2% DME, T_c=980 K

(c) 5% DME, T_c=900 K

(d) pure DME, T_c= 680 K

Figure 6. Measured (markers) and calculated (lines) ignition delay times at φ = 0.5 for NH_3/DME mixtures of different composition. Open symbols are first-stage delay times; filled symbols are overall times. Solid lines-total ignition delay time, dashed lines – first-stage ignition delay time. Data in Fig. 6a are taken from [5].

At φ = 1.0 and 2.0 (Supplementary Material), the calculations and measurements disagree by generally less than 50% for both the overall and first-stage ignition delay times with 5% DME in the fuel. We note that the two-stage ignition cannot be reliably extracted from the

calculation at P_c= 70 bar at φ = 2.0 for 5% DME, resulting in a shoulder similar to that described above. The mechanism predicts the overall ignition delay times of pure DME well, with deviations less than 20%, although it overpredicts the first-stage ignition delay time by a factor of 2 at P_c = 10 bar. We also note the appearance of two-stage ignition in pure DME at pressures below 40 bar, consistent with earlier measurements [34]. Given the lengthening of the first stage relative to the overall ignition delay time shown in Fig. 6d, we expect it to become indistinguishable from the overall delay at higher pressures.

Temperature-dependent ignition delay times at 20 and 40 bar for φ = 1.0 and 5% DME, given in the Supplementary Material, show similar trends as at 60 bar. Here we note that the first stage of ignition is shorter at 20 bar, as compared to the overall delay time. In contrast with the results in Fig. 6c, the mechanism substantially overpredicts the ignition delay time at 20 bar.

3.5 Kinetic analysis and the impact of DME on ammonia ignition

To gain more insight into the effect of DME on ammonia ignition at P_c=60 bar, we consider the kinetics and mechanism of the oxidation process. Mindful of the uncertainties in the mechanism described in Section 2.2.1 above, and with an eye towards identifying potential improvement, we sketch the results of the reaction path and sensitivity analyses, concentrating on those features relevant to the (multi-stage) ignition characteristics. The conditions at φ = 0.5, where the simulations reproduce the slow pressure rise for the DME/NH_3 mixtures in the experiments for 2% DME in the fuel and the "shoulder" from unresolved two-stage ignition in the ignition curves at 5% DME, are used to frame the analysis. The discussion is briefly extended to φ = 1.0, where the mechanism also reasonably replicates overall ignition for both DME fractions and first-stage ignition for 5% DME, to contrast any differences that appear when changing equivalence ratio. For the purposes of comparison, the results for φ = 2.0 are also included in the discussion, despite the structural discrepancy between the computed and measured ignition delay times for pure ammonia mentioned above. In Section 3.5.3, we suggest a picture of how DME exerts its influence on ammonia ignition.

Since the analysis of the mechanisms responsible for the ignition of both ammonia [5,6,12,14,15] and DME [31–34] have been discussed in detail elsewhere, it will not be repeated here. We observe that the reaction path for pure ammonia derived using the current mechanism is essentially identical to that described previously [5,6,12,14,15], including that at φ = 2.0.

3.5.1 Reaction path of NH_3/DME mixtures

Following the methods described in the ignition literature ([5,6,15,32,61] and elsewhere), we consider the reaction path at 20% fuel consumption. The relative changes in the fractions of NH_3 and DME, together with the mixture temperature, are illustrated in Fig. 7 (2% DME, φ = 0.5, T_c= 950 K, P_c= 60 bar). Computed results for conditions exhibiting two-stage ignition show only modest, qualitative, differences with Fig. 7. We first observe that the consumption of the fuel, particularly DME, starts long before ignition, with DME oxidation beginning in the initial milliseconds. At 20% consumption of the total fuel fraction, nearly 90% of the DME has been consumed. A similar early decomposition of DME was also observed in DME/CH_4 mixtures in a flow reactor [37]. As will be discussed below, the early oxidation of DME plays an important role in initiating the oxidation at temperatures well below that at which neat ammonia ignites on the timescale of the experiments. Figure 7 shows that the temperature begins to increase noticeably within the first milliseconds. To gain insight into the apparently phased oxidation of the fuel mixture, we first consider the reaction path for DME in the mixture at 20% DME consumption. We note that the reaction path for ammonia in the DME mixtures studied here shows only modest changes from that reported previously for pure ammonia [5,6]. Since the ammonia fraction at 2% DME and 5% DME is 49 and 19 times higher, respectively, than that of DME, this is to be expected. In contrast, the direct participation of nitrogen-containing species in the oxidation of DME will be seen to have a significant impact on both the reaction path of DME and the ignition process.

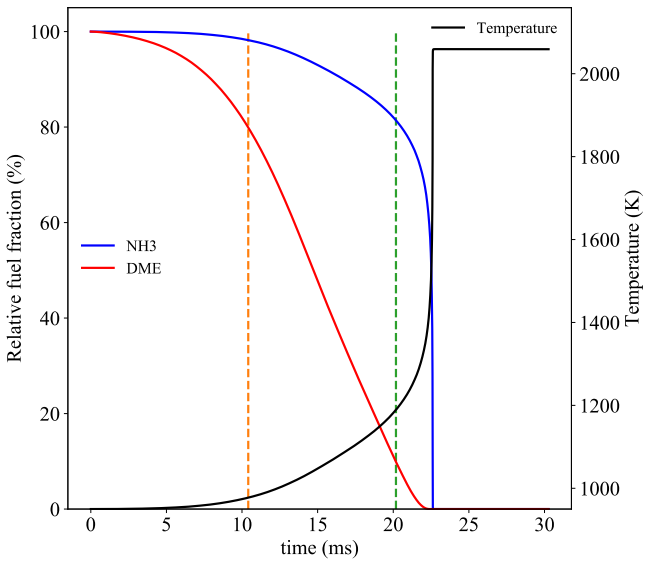

Figure 7. Profiles of relative fractions of DME and NH_3, and the temperature. Conditions: 2% DME, φ = 0.5, T_c = 950 K, P_c = 60 bar. Dashed vertical lines indicate: 20% DME consumption (orange) and 20% total fuel consumption (green).

3.5.1.1 DME path at 20% DME consumption

The reaction path of 2% DME in ammonia at φ = 0.5, T_c = 950 K, P_c = 60 bar is shown in Fig. 8. At 20% DME consumption, roughly 2% of the ammonia has reacted and the mixture temperature T has risen to 977 K. Anticipating the discussion of heat release below, we recall that the 2% ammonia that is consumed is twice the number of molecules as the 20% DME, together causing a 27 K rise in temperature, even at this early stage in the ignition process. We also note that, as can be seen in Fig. 7, significant oxidation of ammonia only occurs above this temperature. As seen in Fig. 8, DME is converted to CH_3OCH_2 primarily by reaction with OH and, interestingly, with NH_2 through reaction R1, above. The analysis shows that half of the CH_3OCH_2 is oxidized via dissociation to CH_3+CH_2O or by reaction with O_2 to produce $2CH_2O$+OH (with more or less equal rates). The current mechanism also predicts that half the methoxymethyl is oxidized through the low-temperature sequence [37] indicated in Fig. 8: reaction of CH_3OCH_2 with O_2 to form CH_3OCH_2OO, isomerization to CH_2OCH_2OOH, oxygen addition to produce $O_2CH_2OCH_2O_2H$, followed by the chain-branching sequence $O_2CH2OCH2O_2H \rightarrow HO_2CH_2OCHO \rightarrow OCH_2OCHO$ producing two OH radicals. We also note that the presence of ammonia results in opening the channel from CH_3OCH_2OO to CH_3OCH_2O, by reaction with NH_2 and NO (via reactions R7 and R8 in Table 2). The CH_3OCH_2O is ultimately converted to methyl formate (CH_3OCHO); while this species is not oxidized further at this point in time, it is ultimately converted to CH_3OCO, which dissociates to CH_3 and CO_2, and CH_2OCHO, and subsequently reacting to CH_2O and HCO. CH_2O is primarily converted to HCO by NH_2, which further is oxidized to CO.

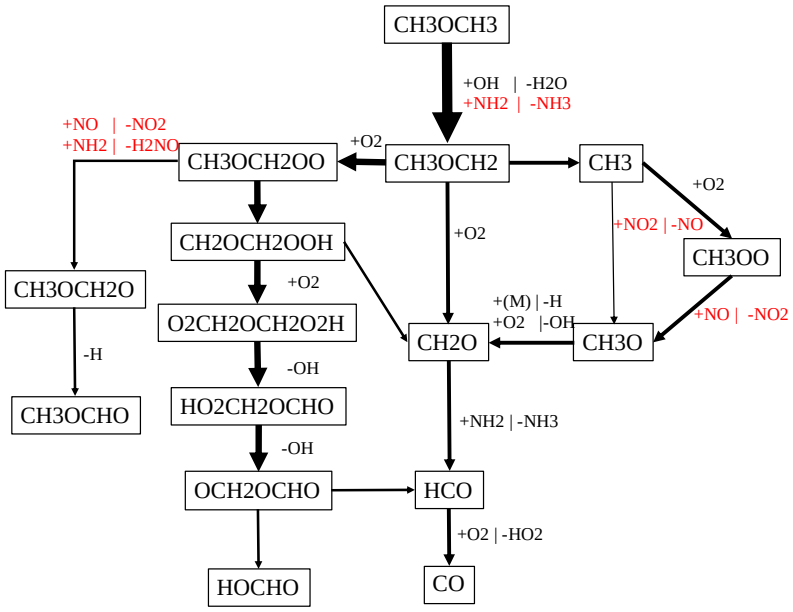

Figure 8. Reaction path diagram of DME in mixture with 2%DME in the fuel at φ = 0.5, T_c= 950 K, P_c = 60 bar at the moment of 20% DME consumption. Species in red denote nitrogen-containing reaction partners and products. The thickness of the arrows are roughly proportional to the flux in the individual steps.

Increasing the DME fraction to 5% of the fuel under the same conditions of φ, T_c and P_c, where 20% oxidation of the DME has resulted in T=985 K, gives nearly an identical path to that in Fig. 8. With the exception of slightly more of the DME being converted to CH_3 and CH_2O, the mechanism predicts an increase in the fraction of CH_3OCH_2OO being converted to methyl formate, from 10% at 2% DME to 27% at 5% DME. We also remark that reactions involving nitrogen-containing species (specifically, NO, H_2NO and NO_2) are involved in the oxidation of CH_3 and CH_3OO, as observed in NH_3/CH_4 mixtures [6].

As shown in Fig. 4, above, increasing the DME fraction from 2% to 5% has such a large effect on the ignition delay time that the entire curve is shifted to lower temperatures. Consequently, it is illustrative to consider the different DME fractions at different temperatures, where they have comparable delay times. This comparison also mirrors the discussion derived from flow reactor data [37]. We contrast the reaction path for 5% DME at T_c=850 K, where the ignition delay time is comparable (~20 ms) to that of 2% DME at 950 K. At 20% DME consumption (where 2.5% of the ammonia has reacted and heat release has increased the mixture temperature to 891 K), the analysis shows that, while the overall oxidation route is similar to that at T_c=950 K, now ~86% of the methoxymethyl reacts via oxygen addition to CH_3OCH_2OO (compared to ~50% at T_c=950 K), of which 67% now proceeds through CH_2OCH_2OOH, while 33% reacts with NH_2 and NO (as noted above) to CH_3OCH_2O and further to methyl formate.

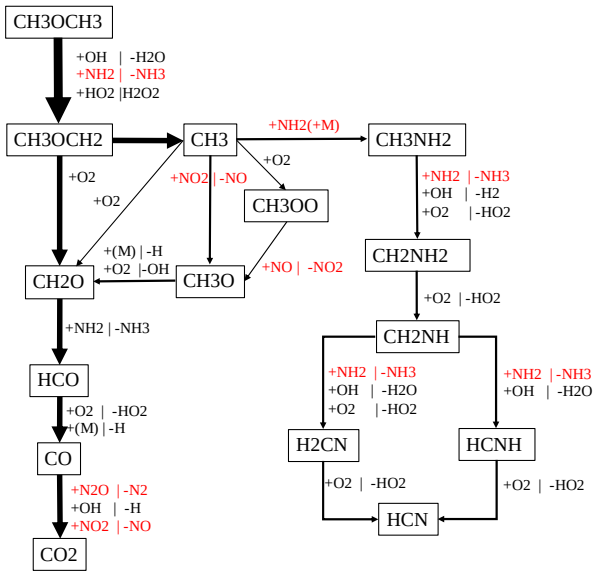

Figure 9. Reaction path diagram of DME in mixture with 2%DME in the fuel at φ = 0.5, T_c=950 K, P_c=60 bar at the moment of 20% total fuel consumption. Species in red denote nitrogen-containing reaction partners and products. The thickness of the arrows are roughly proportional to the flux in the individual steps.

3.5.1.2 DME path at 20% fuel consumption and other equivalence ratios

At 20% total fuel consumption, the reaction path has shifted considerably, as shown in Fig. 9. For 2% DME at T_c=950 K, where the mixture temperature is now 1189 K, the path via CH_3OCH_2OO has all but disappeared, with all the CH_3OCH_2 being oxidized via dissociation or reaction with O_2 to form two formaldehyde molecules and a hydroxyl radical, both accounting for half the consumption of the methoxymethyl radical. At this higher mixture temperature, the oxidation of the methyl radical is now dominated by nitrogen-containing species, with roughly equal quantities reacting via $CH_3 + NO_2 \rightarrow CH_3O + NO$ and $CH_3 + NH_2 (+M) \rightarrow CH_3NH_2 (+M)$. Methoxy reacts to formaldehyde, primarily by dissociation. Methylamine reacts further along the route: $CH_3NH_2 \rightarrow CH_2NH_2 \rightarrow CH_2NH \rightarrow H_2CN/HCNH \rightarrow HCN$. Increasing the DME fraction to 5% at the same T_c shows only marginal differences. At 5% DME and T_c=850 K (T=1106 K at 20% fuel consumption), the computations show 10% of the methoxymethyl radical still being oxidized through CH_3OCH_2OO.

The reaction paths at φ = 1.0, T_c=950 K, P_c=60 bar, at 20% DME consumption, show no new features as compared to those at φ = 0.5 discussed above, with the exception of a significant amount of methane at 20% fuel consumption; this is formed from the methyl radical produced from the thermal dissociation of methoxymethyl. In addition, at 20% total fuel consumption, DME undergoes thermal dissociation to produce CH_3 and CH_3O directly, which is not observed at φ = 0.5. The dissociation of DME and methoxymethyl favors the routes to

CH_3O, CH_3 and CH_2O at the expense of the low-temperature route. At 20% DME consumption, for 2% and 5% DME at T_c=950 K, the lower oxygen fraction at φ = 1.0 results in ~38% less $O_2CH2OCH2O_2H$ being formed than at φ = 0.5. Under these conditions, oxidation paths of methoxymethyl (Fig. 8) involving less molecular oxygen, such as to CH_2O (one O_2) or CH_3 (none) are expected to be favored as compared to the route from CH_3OCH_2 to $O_2CH2OCH2O_2H$, which requires two oxygen molecules. This shift is smaller (~25% less $O_2CH2OCH2O_2H$) for 5% DME and T_c=850 K. At φ = 2.0, the shift towards methane and formaldehyde as dominant intermediates continues. We also note that at this equivalence ratio the computations predict that there is substantial residual ammonia after ignition.

We identify the steady increase in temperature observed numerically for all conditions, caused by the early consumption of the fuel illustrated in Fig. 7, as the origin of the increase in post-compression pressure observed experimentally. The early oxidation of DME at these temperatures, which would result in rapid ignition in pure DME (<1 ms at high pressure [31]), suggests itself as the cause of the heat release during compression observed in some of the experiments. The development of heat release in the pre-ignition period will be discussed in Section 3.5.3. While the dominance of the low-temperature route in the ignition of the ammonia/DME mixtures studied here also suggests the attendant chain branching, itself, as the cause of two-stage ignition in these mixtures, the very low fractions of DME in these experiments make this notion seem unlikely (see also Section 3.5.3). However, the path by which DME generates reactive species needed to decompose NH_3 is certainly important for understanding the details of DME-induced ignition in ammonia. Further consideration of the rates in different parts of the mechanism may improve the ability to predict the slow pressure rise and two-stage ignition under the conditions studied here. The discussion in Section 2.2.1 and the result shown above suggest reactions of DME with NO_x species, reactions leading to the distribution of products arising from methoxymethyl, and ammonia-specific reactions diverting CH_3OCH_2OO from the low-temperature chain-branching reactions (resulting in methyl formate as described above) as candidates.

3.5.1.3 NH_3 path at 20% fuel consumption

Regarding the reaction path of ammonia, whose major fluxes at 20% fuel consumption are nearly identical to those of pure ammonia under the conditions of pressure, temperature and equivalence ratio at which it ignites [5,6] (included in the Supplementary Material), we observe that the vast majority of the reactions with C-containing species are only a few percent of the

flux at any given point. As observed for the admixture of hydrogen [5,15] and methane [6], the major reactions for production of the species relevant for oxidation and ignition of ammonia with DME, i.e., OH, HO_2 and H_2O_2, do not change dramatically, but their rates do. This is illustrated in Fig. 10, which shows the ROP for OH production for pure ammonia and 5% DME at φ= 0.5, P_c=60 bar and T_c=950 K (ROPs for HO_2 and H_2O_2 at these and other conditions are included in the Supplementary Material). The ROP shows that the dominant reactions for OH production in the pre-ignition period (taking the trajectory between T_c and 1200 K for this purpose [6]), $HO_2+NO \rightarrow OH+NO_2$, $HO_2+NH_2 \rightarrow H_2NO+OH$, $NH_2+NO \rightarrow NNH+OH$ and $HONO \rightarrow NO+OH$, remain dominant for DME admixture, but increase much more rapidly with temperature than in neat NH_3. This points to the importance of DME oxidation for accelerating ammonia decomposition. At 1200 K, 5% DME in the fuel increases the rates of these reactions by a factor of 10-20. The magnitude of the increases in rate at 5% DME observed here is similar to those seen for 50% methane in ammonia [6]. Nearly all the OH is consumed by $NH_3+OH \rightarrow NH_2+H_2O$, with a small contribution from $CH_3OCH_3+OH \rightarrow CH_3OCH_2+H_2O$, keeping the OH fraction low until ignition. We note that the variation in the rates in Fig. 10 (right) between 1100 K and 1200 K is due to the "shoulder" in the computed temperature profile; the two major reactions continue their sharp increase with temperature above 1200 K.

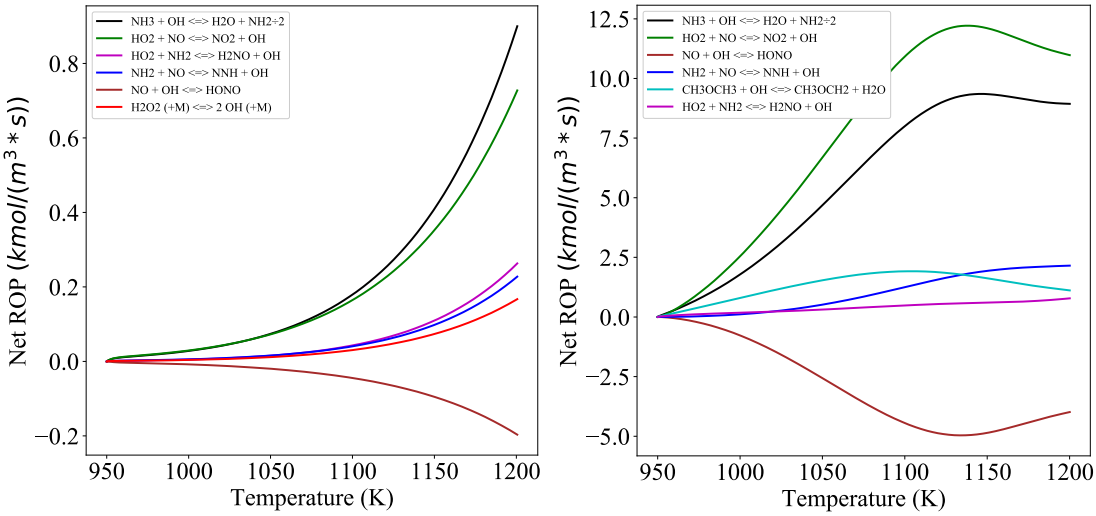

Figure 10. Rate-Of-Production analysis for OH production for pure ammonia (left) and 5% DME (right) at φ= 0.5, P_c=60 bar and T_c=950 K. Note that the rate of production for NH_3+OH has been divided by 2.

Recalling the temporal development of fuel consumption and temperature rise in Fig. 7, above, the computations also show that in the initial milliseconds, the low-temperature chain-branching sequence is the major source of OH, initiating the decomposition of NH_3, but being rapidly overtaken by $HO_2+NO \rightarrow OH+NO_2$. As a result, the early rate of $NH_3+OH \rightarrow NH_2+H_2O$

at T_c= 950 K is ten times higher than for ammonia under the same conditions, while for T_c= 850 K, pure ammonia at φ = 0.5 is not reactive on the time scale of ignition.

3.5.2 Sensitivity analysis

The sensitivity analysis for ignition delay time, based on the mechanism presented here, is shown in Fig. 11 for the three sets of conditions described above. We first remark that at both 2% and 5% DME four of the most important reactions are identical to those of pure ammonia at 1000 K reported previously [6], all involving NH_2 and NO/NO_2. A notable exception, $HO_2+NH_2 \rightarrow NH_3+O_2$ (R1b) now appears as one of the most inhibiting reactions for all three mixtures, after inclusion of the fast rate constant calculated by Stagni et al. [38]. The most striking effect of DME admixture on the sensitivity is the introduction of two reactions that compete for OH: the enhancing reaction $CH_3OCH_3+OH \rightarrow CH_3OCH_2+H_2O$, initiating the decomposition of DME, and $NH_3+OH \rightarrow H_2O+NH_2$ that inhibits ignition. At 5% DME and T_c=850 K, these reactions dominate the sensitivity. While the ROP, above, indicates that NH_3+OH is always the dominant pre-ignition OH-consuming reaction, this reaction does not occur in previous sensitivity analyses for the ignition delay time for pure NH_3 at temperatures extant in an RCM [5,6,15]. The reaction was reported in the sensitivity analyses for OH fraction for φ= 2.0 taken at 1% ammonia consumption under RCM conditions in [38], but it does not appear in the sensitivity analyses for pure ammonia performed using the current mechanism (see Supplementary Material). This competition underlines the importance of OH for promoting ignition by initiating the decomposition of DME. The parallel step for decomposing the fuel, by $CH_3OCH_3+NH_2 \rightarrow CH_3OCH_2+NH_3$, shows substantial sensitivity as stated in Section 2.2.1 above, but is relatively insensitive to the DME fraction in the fuel. Further, we observe three reactions that have been identified as dominant reactions in the sensitivity analysis for pure DME [32]. The inhibiting reactions $CH_3OCH_2 \rightarrow CH_2O+CH_3$ and $CH_2OCH_2OOH \rightarrow 2CH_2O+OH$ compete with $CH_2OCH_2OOH+O_2 \rightarrow O_2CH2OCH2O_2H$, which leads to low-temperature chain branching as discussed above. Also notable is that the reaction $CH_3OCH_2OO+NO \rightarrow CH_3OCH_2O+NO_2$, which was seen above to be an important diversion from isomerization to CH_2OCH_2OOH and the further chain-branching reactions, reaches 20% sensitivity for 5% DME at 850 K, also pointing to the importance of the low-temperature path for ignition under these conditions. Despite the very low fraction of DME in the fuel, it is noteworthy that reactions related to DME oxidation, and particularly those related to low-temperature chain branching, show such relative importance for the ignition delay time in ammonia mixtures. A similar observation on the importance of DME chemistry has been

made regarding the effect of DME addition on methane ignition [32], but at DME fractions that are 4-10 times higher than those considered here.

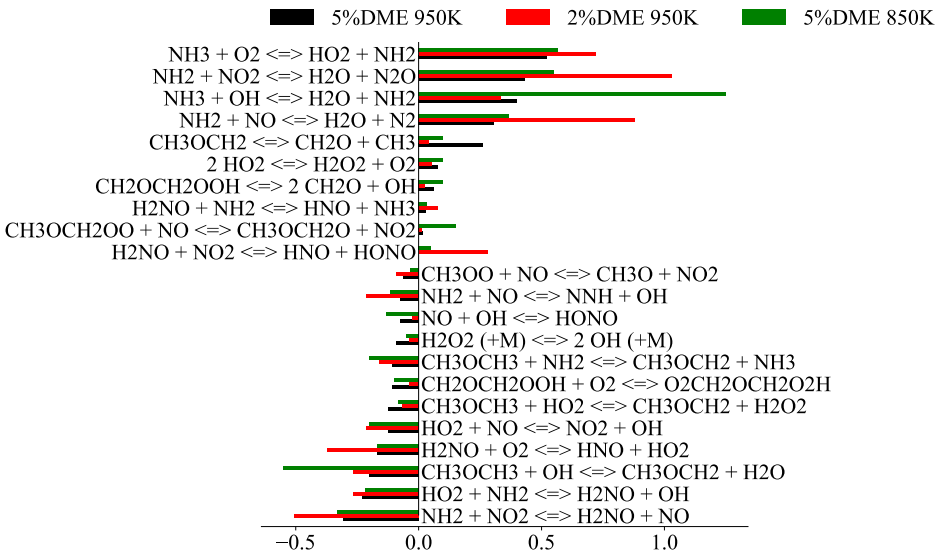

Figure 11. Sensitivity analysis for ignition delay time of DME/NH_3 mixture at P_c=60 bar and φ = 0.5, for 2% DME at T_c=950 K and 5% DME at T_c=950 and 850 K.

The changes in the sensitivity analysis upon varying the equivalence ratio are illustrated in Fig. 12, for 5% DME at P_c=60 bar, T_c=850 K and φ = 0.5, 1.0 and 2.0. With the exception of the minor decrease in the sensitivity of the ignition delay time to NH_3+OH → H_2O+NH_2, there is essentially no change to the important reactions as a function of equivalence ratio. Given that the measured overall ignition delay time has been seen to be nearly insensitive to equivalence ratio (Fig. 5c) and that under these conditions the experimental results are well predicted by the mechanism used here, the sensitivity analysis suggests that there is no substantial change in the identity of the dominant reactions that maintain the ignition delay time upon decreasing the oxygen fraction in the fuel.

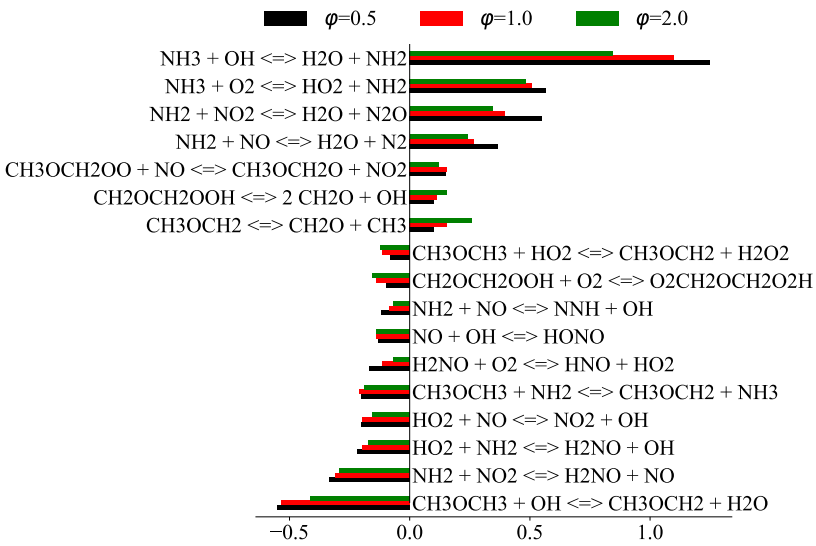

Figure 12. Sensitivity analysis of NH_3 with 5% DME at T_c=850 K, P_c=60 bar, and φ = 0.5, 1.0 and 2.0.

3.5.3 Species profiles and heat release

To complete the discussion of the mechanism through which DME accelerates ammonia ignition, we examine the computed species and heat-release time histories for 5% DME in ammonia, T_c=850 K, P_c=60 bar, and φ = 0.5 in Fig. 13. The two vertical dashed lines indicate 20% DME consumption at T=891 K and 20% total fuel consumption at T=1106 K, as indicated above. In previous reports, we discussed the promoting effects of H_2 [5] and CH_4 [6] on ammonia ignition in terms of the orders-of-magnitude increase in pre-ignition fractions of HO_2 and H_2O_2 as compared to pure ammonia under the same conditions. The analysis of the effects of DME using the current mechanism, however, suggests that the buildup of H_2O_2, similar to the description of hydrocarbon ignition [64], is less relevant for ignition of the NH_3/DME mixtures studied here. Referring to Fig. 13a, whereas there is a significant buildup of H_2O_2, the oxidation of this species begins well before the first stage of ignition, having reached its maximum fraction at the same time at which DME is only 20% consumed, rather than immediately prior to ignition as for H_2 and CH_4 additives.

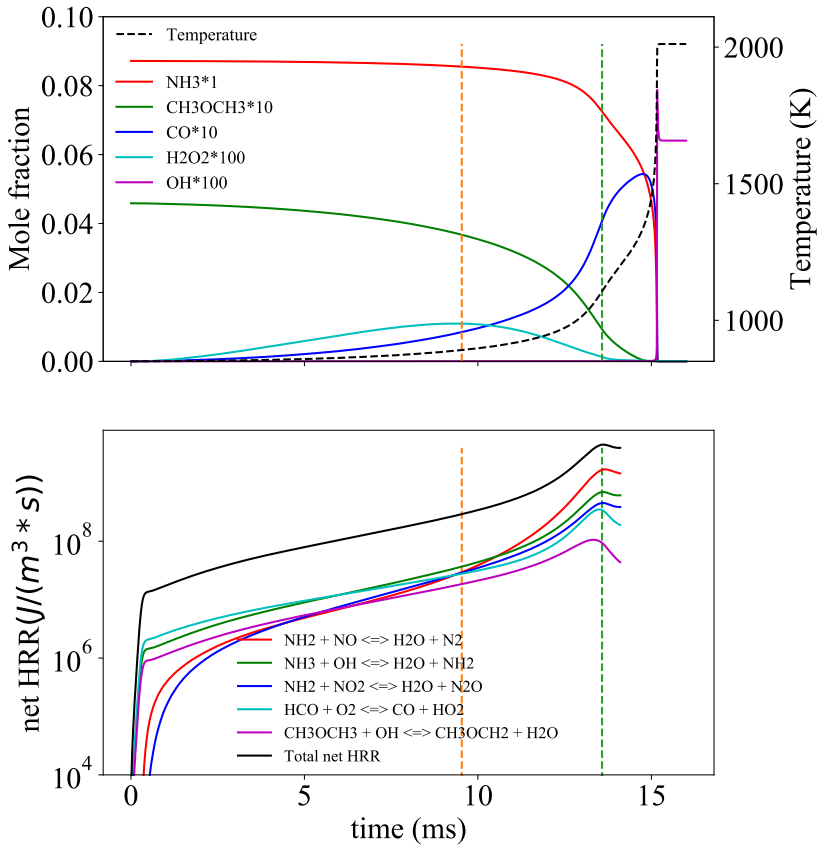

Figure 13. Computed time histories of selected species and temperature (a) and net heat release rate (HRR) (b). The vertical dashed lines indicate 20% DME consumption at 891 K (orange) and 20% total fuel consumption at 1106 K (green). Conditions: 5% DME, T_c=850 K, P_c=60 bar, φ = 0.5. The heat release curves are computed up to 1200 K.

Since the effects of DME are intimately related to the substantial pre-ignition heat release, we examine the reactions that generate heat between compression and (overall) ignition. The heat release between T_c and 1200 K is given in Fig. 13b, for the total heat release and the heat release from a number of the most important contributing reactions. In the first few milliseconds, the reactions $NH_3+OH \rightarrow H_2O+NH_2$, $HCO+O_2 \rightarrow CO+HO_2$ and $CH_3OCH_3+OH \rightarrow CH_3OCH_2+H_2O$ generate the most heat. By roughly 5 ms, the contribution from these reactions is equaled by $NH_2+NO_2 \rightarrow H_2O+N_2O$ and $NH_2+NO \rightarrow H_2O+N_2$. The importance of the latter reaction grows rapidly from ~10 ms; by ~13 ms NH_2+NO has become the dominating reaction in the heat release by a factor of 2. Obviously, the contribution from the reaction of $CH_3OCH_3+OH \rightarrow CH_3OCH_2+H_2O$ is limited as compared to that from species derived from ammonia, since its initial concentration is 19 times lower than that of ammonia and by 13 ms the actual mole fraction of DME has been depleted by 90%. Please note that the apparent maximum in all the heat release curves at roughly 13 ms (coincidentally coinciding with the vertical dashed line showing 20% total fuel consumption) is caused by the “shoulder”

in the temperature history, equivalent to the first stage ignition described above. The reactions involving NH_3 and NH_2 increase rapidly again within 1 ms, as the mixture approaches overall ignition at slightly more than 15 ms. Since the DME is nearly exhausted, the contributions from DME and HCO to the heat release decrease after ~13 ms, as indicated in the profiles of DME and CO in Fig. 13a. A somewhat paradoxical observation is that the three major heat-releasing reactions are also three of the most important ignition-inhibiting reactions shown in the sensitivity analyses in Figs. 11 and 12, above. While the heat release is clearly necessary to accelerate the reactions leading to ignition, kinetically, these reactions appear to retard ignition.

Analogous to the observation regarding the importance of the low-temperature route for DME oxidation in generating OH in the first few milliseconds, Fig. 13b also shows the equivalent contribution of the decomposition of DME to the initial heat release. Similarly, the rapid increase of the rates of reactions in the ammonia submechanism itself, once initiated by DME decomposition, is reflected in the rapid dominance of these reactions in the heat release. Particularly interesting in this regard is the rapid increase in the contribution from $NH_2+NO \rightarrow H_2O+N_2$ to heat release, whose growth (note the logarithmic scale) corresponds well with the shoulder in the temperature history seen in Fig. 13a. This suggests a relation with a first ignition stage, as well as a minimum temperature rise necessary to accelerate heat release (in this numerical case ~50 K). While this growth in heat release also follows the decrease in the DME fraction, we report that the rate of OH formation from DME oxidation is more than 15 times lower than that from $HO_2+NO \rightarrow OH+NO_2$. Consequently, under these conditions the current mechanism suggests that any contribution from DME oxidation to two-stage ignition in these mixtures is indirect. Preliminary examination of the origin and effect of heat release at other equivalence ratios indicates similar phenomena. Improvements to the mechanism that result in a more faithful quantitative reproduction of the slow pressure rise and two-stage ignition observed in the experiments will permit the determination of the physical-chemical origins of this behavior.

The overall picture that emerges from the analysis is that, even at very low fractions (2-5%) of DME in the fuel, the reactions of DME generate enough heat and reactive species to initiate the oxidation of ammonia, and thus facilitate ignition at temperatures after compression that are hundreds of degrees lower than that for ammonia without DME addition.

4. Summary and Conclusions

At high pressure, very low fractions of DME admixed with ammonia (2-5% in the fuel) shorten the ignition delay time by more than an order of magnitude. These low fractions effectively shift the curves of ignition delay time vs. temperature at constant pressure. At a constant ignition delay time, 2% DME shifts the ignition curve by ~150 K, while 5% DME shifts the curve by roughly 250 K. Thus, DME admixture allows ignition of the ammonia-based fuel at temperatures far removed from those at which neat ammonia would ignite at the same pressure. This property makes it potentially attractive as a combustion-enhancing additive for ammonia as a fuel. Two-stage ignition is observed at φ=1.0 and 2.0 with 2% and 5% DME in the fuel, despite the very low DME fraction in the combustible mixture (<1%) and the pressure being higher than that at which pure DME shows two-stage ignition. At φ=0.5, a reproducible pre-ignition pressure rise is observed for both DME fractions, which is not observed in the pure fuel components. The equivalent heat release of the first-stage ignition and the slow pressure rise are both roughly 100 K as compared to the temperature that would exist in a non-reactive mixture. This rise in temperature is seen to be an important aspect of the ignition-enhancing effect of DME on ammonia.

The chemical mechanism presented here, which contains several new reactions describing interaction between DME and ammonia species, as well as a number of revised reactions in the ammonia submechanism, captures the pre-ignition slow temperature rise for the ammonia/DME mixtures faithfully; while the mechanism exhibits two-stage ignition, both qualitative and quantitative improvement is recommended. The modified mechanism also predicts the ignition of pure ammonia at φ=0.5 and 1.0 as well or better than the original mechanism, but at φ=2.0 it is less accurate than the original. The overall ignition delay times for ammonia/DME mixtures are predicted well, generally being within 50% of the experimental values. Simulating the ignition process using the mechanism, we observe that the DME is oxidized much more rapidly than ammonia, with ~90% of the DME being already oxidized at the time at which 20% of the total fuel (DME+NH_3) has been consumed. Analysis of the mechanism indicates that this ‘early DME oxidation’ generates reactive species that initiate the oxidation of ammonia, which in turn begins heat release, further accelerating the oxidation process and resulting in ignition. The reaction path analysis shows that the low-temperature chain-branching reactions of DME are important in the early oxidation of the fuel. The sensitivity analysis shows further that a number of these reactions of DME are important for ignition, even at fractions of 2% in the fuel. Consideration of the reactions responsible for

heat release in the pre-ignition period suggests that first-stage heat release occurs via reactions of nitrogen containing species, but is initiated by early heat release and OH formation from DME oxidation. Further examination of the distribution of products arising from methoxymethyl, of the ammonia-specific reactions involving CH_3OCH_2OO or other species derived from DME, as well as reactions between DME and NO_x, may improve the mechanism's ability to predict two-stage ignition under the conditions studied here.

Acknowledgments

The authors would like to thank one of the reviewers for pointing out the potential importance of the DME+NO_2 reaction. L. Dai thanks the China Scholarship Council (CSC) for the financial support. P.G. would like to acknowledge funding from Orient's Fund and Innovation Fund Denmark. P.M. acknowledges support from the US Department of Energy, Grant DESC0020952.

References

[1] E. Kroch, Ammonia- A Fuel for Motor Buses, J. Inst. Pet. 31 (1945) 213–223.

[2] R. Seaman, G. Huson, The choice of NH_3 to fuel the X-15 Rocket plane, NH_3 Assoc. (2011).

[3] K. Takizawa, A. Takahashi, K. Tokuhashi, S. Kondo, A. Sekiya, Burning velocity measurements of nitrogen-containing compounds, J. Hazard. Mater. 155 (2008) 144–152.

[4] H. Kobayashi, A. Hayakawa, K.D.K.A. Somarathne, E.C. Okafor, Science and technology of ammonia combustion, Proc. Combust. Inst. 37 (2019) 109–133.

[5] L. Dai, S. Gersen, P. Glarborg, H. Levinsky, A. Mokhov, Experimental and numerical analysis of the autoignition behavior of NH_3 and NH_3/H_2 mixtures at high pressure, Combust. Flame. 215 (2020) 134–144.

[6] L. Dai, S. Gersen, P. Glarborg, A. Mokhov, H. Levinsky, Autoignition studies of NH_3/CH_4 mixtures at high pressure, Combust. Flame. 218 (2020) 19–26.

[7] O. Kurata, N. Iki, T. Matsunuma, T. Inoue, T. Tsujimura, H. Furutani, H. Kobayashi, A. Hayakawa, Performances and emission characteristics of NH_3–air and NH_3/CH_4–air combustion gas-turbine power generations, Proc. Combust. Inst. 36 (2017) 3351–3359.

[8] A.J. Reiter, S.C. Kong, Demonstration of compression-ignition engine combustion using ammonia in reducing greenhouse gas emissions, Energy and Fuels. 22 (2008) 2963–2971.

[9] A.J. Reiter, S.C. Kong, Combustion and emissions characteristics of compression-ignition engine using dual ammonia-diesel fuel, Fuel. 90 (2011) 87–97.

[10] C.W. Gross, S.C. Kong, Performance characteristics of a compression-ignition engine using direct-injection ammonia-DME mixtures, Fuel. 103 (2013) 1069–1079.

[11] K. Ryu, G.E. Zacharakis-Jutz, S.C. Kong, Performance characteristics of compression-ignition engine using high concentration of ammonia mixed with dimethyl ether, Appl. Energy. 113 (2014) 488–499.

[12] O. Mathieu, E.L. Petersen, Experimental and modeling study on the high-temperature oxidation of Ammonia and related NO_x chemistry, Combust. Flame. 162 (2015) 554–570.

[13] B. Shu, S.K. Vallabhuni, X. He, G. Issayev, K. Moshammer, A. Farooq, R.X. Fernandes, A shock tube and modeling study on the autoignition properties of ammonia at intermediate temperatures, Proc. Combust. Inst. 37 (2019) 205–211.

[14] M. Pochet, V. Dias, B. Moreau, F. Foucher, H. Jeanmart, F. Contino, Experimental and numerical study, under LTC conditions, of ammonia ignition delay with and without hydrogen addition, Proc. Combust. Inst. 37 (2018) 621–629.

[15] X. He, B. Shu, D. Nascimento, K. Moshammer, M. Costa, R.X. Fernandes, Auto-ignition kinetics of ammonia and ammonia/hydrogen mixtures at intermediate temperatures and high pressures, Combust. Flame. 206 (2019) 189–200.

[16] A.A. Konnov, J. De Ruyck, A possible new route for no formation via N_2H_3, Combust. Sci. Technol. 168 (2001) 1–46.

[17] Y. Zhang, O. Mathieu, E.L. Petersen, G. Bourque, H.J. Curran, Assessing the predictions of a NO_x kinetic mechanism on recent hydrogen and syngas experimental data, Combust. Flame. 182 (2017) 122–141.

[18] Y. Song, H. Hashemi, J.M. Christensen, C. Zou, P. Marshall, P. Glarborg, Ammonia oxidation at high pressure and intermediate temperatures, Fuel. 181 (2016) 358–365.

[19] P. Dagaut, A. Nicolle, Experimental and kinetic modeling study of the effect of SO_2 on the reduction of NO by ammonia, Proc. Combust. Inst. 30 (2005) 1211–1217.

[20] H. Nakamura, S. Hasegawa, T. Tezuka, Kinetic modeling of ammonia/air weak flames in a micro flow reactor with a controlled temperature profile, Combust. Flame. 185

(2017) 16–27.
[21] P. Glarborg, J.A. Miller, B. Ruscic, S.J. Klippenstein, Modeling nitrogen chemistry in combustion, Prog. Energy Combust. Sci. 67 (2018) 31–68.
[22] S.J. Klippenstein, L.B. Harding, P. Glarborg, J.A. Miller, The role of NNH in NO formation and control, Combust. Flame. 158 (2011) 774–789.
[23] K.P. Shrestha, L. Seidel, T. Zeuch, F. Mauss, Detailed Kinetic Mechanism for the Oxidation of Ammonia Including the Formation and Reduction of Nitrogen Oxides, Energy and Fuels. 32 (2018) 10202–10217.
[24] U. of C. at S.D. Mechanical and Aerospace Engineering (Combustion Research), Chemical-Kinetic Mechanisms for Combustion Applications, http://web.eng.ucsd.edu/mae/groups/combustion/mechanism.html, (2014).
[25] Z. Tian, Y. Li, L. Zhang, P. Glarborg, F. Qi, An experimental and kinetic modeling study of premixed $NH_3/CH_4/O_2$/Ar flames at low pressure, Combust. Flame. 156 (2009) 1413–1426.
[26] R. Li, A.A. Konnov, G. He, F. Qin, D. Zhang, Chemical mechanism development and reduction for combustion of $NH_3/H_2/CH_4$ mixtures, Fuel. 257 (2019) 116059.
[27] E.C. Okafor, Y. Naito, S. Colson, A. Ichikawa, T. Kudo, A. Hayakawa, H. Kobayashi, Experimental and numerical study of the laminar burning velocity of CH_4–NH_3–air premixed flames, Combust. Flame. 187 (2018) 185–198.
[28] L. Yu, Y. Feng, W. Wang, J. Zhu, Y. Qian, X. Lu, Combustion and Flame The effect of ammonia addition on the low-temperature autoignition of n-heptane : An experimental and modeling study, Combust. Flame. 217 (2020) 4–11.
[29] K. Zhang, C. Banyon, J. Bugler, H.J. Curran, A. Rodriguez, O. Herbinet, F. Battin-Leclerc, C. B'Chir, K.A. Heufer, An updated experimental and kinetic modeling study of n-heptane oxidation, Combust. Flame. 172 (2016) 116–135.
[30] M.Y. Kim, S.H. Yoon, B.W. Ryu, C.S. Lee, Combustion and emission characteristics of DME as an alternative fuel for compression ignition engines with a high pressure injection system, Fuel. 87 (2008) 2779–2786.
[31] H.J. Curran, W.J. Pitz, C.K. Westbrook, P. Dagaut, J.-C. Boettner, M. Cathonnet, A Wide Range Modeling Study of Dimethyl Ether Oxidation, Int. J. Chem. Kinet. 30 (1998) 229–241.
[32] U. Burke, K.P. Somers, P. O'Toole, C.M. Zinner, N. Marquet, G. Bourque, E.L. Petersen, W.K. Metcalfe, Z. Serinyel, H.J. Curran, An ignition delay and kinetic modeling study of methane, dimethyl ether, and their mixtures at high pressures, Combust. Flame. 162 (2015) 315–330.
[33] E.E. Dames, A.S. Rosen, B.W. Weber, C.W. Gao, C.-J. Sung, W.H. Green, A detailed combined experimental and theoretical study on dimethyl ether/propane blended oxidation, Combust. Flame. 168 (2016) 310–330.
[34] G. Mittal, M. Chaos, C.-J. Sung, F.L. Dryer, Dimethyl ether autoignition in a rapid compression machine: Experiments and chemical kinetic modeling, Fuel Process. Technol. 89 (2008) 1244–1254.
[35] H. Wang, R. Fang, B.W. Weber, C.-J. Sung, An experimental and modeling study of dimethyl ether/methanol blends autoignition at low temperature, Combust. Flame. 198 (2018) 89–99.
[36] H. Wu, Z. Shi, C. Lee, H. Zhang, Y. Xu, Experimental and kinetic study on ignition of DME/n-butane mixtures under high pressures on a rapid compression machine, Fuel. 225 (2018) 35–46.
[37] H. Hashemi, J.M. Christensen, P. Glarborg, High-pressure pyrolysis and oxidation of DME and DME/CH_4, Combust. Flame. 205 (2019) 80–92.
[38] A. Stagni, C. Cavallotti, S. Arunthanayothin, Y. Song, O. Herbinet, F. Battin-Leclerc,

T. Faravelli, An experimental, theoretical and kinetic-modeling study of the gas-phase oxidation of ammonia, React. Chem. Eng. 5 (2020) 696–711.
[39] S. Gersen, A. V. Mokhov, J.H. Darmeveil, H.B. Levinsky, Ignition properties of n-butane and iso-butane in a rapid compression machine, Combust. Flame. 157 (2010) 240–245.
[40] S. Gersen, A. V. Mokhov, J.H. Darmeveil, H.B. Levinsky, P. Glarborg, Ignition-promoting effect of NO_2 on methane, ethane and methane/ethane mixtures in a rapid compression machine, Proc. Combust. Inst. 33 (2011) 433–440.
[41] P. Park, J.C. Keck, Rapid Compression Machine Measurements of Ignition Delays for Primary Reference Fuels, in: SAE Tech. Pap., SAE International, 1990.
[42] S. Gersen, Experimental study of the combustion properties of methane / hydrogen mixtures, Ph.D. Thesis, University of Groningen,http://hdl.handle.net/11370/8161b901-4e2b-40dd-8140-c926a9243a4e, 2007.
[43] S.G. Cheskis, O.M. Sarkisov, Flash photolysis of ammonia in the presence of oxygen, Chem. Phys. Lett. 62 (1979) 72–76.
[44] V.A. Lozovskii, V.A. Nadtochenko, O.M. Sarkisov, S.G. Cheskis, Study of NH_2 radical recombination by intraresonator laser spectroscopy, Kinet. Catal. 20 (1979) 918–922.
[45] X. Chen, M.E. Fuller, C. Franklin Goldsmith, Decomposition kinetics for HONO and HNO_2, React. Chem. Eng. 4 (2019) 323–333.
[46] J. Gao, Y. Guan, J. Lou, H. Ma, J. Song, Kinetic modeling for unimolecular B-scission of the methoxymethyl radical from quantum chemical and RRKM analyses, Combust. Flame. (2018).
[47] M.J. Frisch, G.W. Trucks, H.B. Schlegel, G.E. Scuseria, M. a. Robb, J.R. Cheeseman, G. Scalmani, V. Barone, G. a. Petersson, H. Nakatsuji, X. Li, M. Caricato, a. V. Marenich, J. Bloino, B.G. Janesko, R. Gomperts, B. Mennucci, H.P. Hratchian, J. V. Ortiz, a. F. Izmaylov, J.L. Sonnenberg, Williams, F. Ding, F. Lipparini, F. Egidi, J. Goings, B. Peng, A. Petrone, T. Henderson, D. Ranasinghe, V.G. Zakrzewski, J. Gao, N. Rega, G. Zheng, W. Liang, M. Hada, M. Ehara, K. Toyota, R. Fukuda, J. Hasegawa, M. Ishida, T. Nakajima, Y. Honda, O. Kitao, H. Nakai, T. Vreven, K. Throssell, J. a. Montgomery Jr., J.E. Peralta, F. Ogliaro, M.J. Bearpark, J.J. Heyd, E.N. Brothers, K.N. Kudin, V.N. Staroverov, T. a. Keith, R. Kobayashi, J. Normand, K. Raghavachari, a. P. Rendell, J.C. Burant, S.S. Iyengar, J. Tomasi, M. Cossi, J.M. Millam, M. Klene, C. Adamo, R. Cammi, J.W. Ochterski, R.L. Martin, K. Morokuma, O. Farkas, J.B. Foresman, D.J. Fox, G16_a03, (2016) Gaussian 16, Revision A.03, Gaussian, Inc., Wallin.
[48] Y. Zhao, D.G. Truhlar, The M06 suite of density functionals for main group thermochemistry, thermochemical kinetics, noncovalent interactions, excited states, and transition elements: Two new functionals and systematic testing of four M06-class functionals and 12 other function, Theor. Chem. Acc. 120 (2008) 215–241.
[49] I.M. Alecu, J. Zheng, Y. Zhao, D.G. Truhlar, Computational Thermochemistry: Scale Factor Databases and Scale Factors for Vibrational Frequencies Obtained from Electronic Model Chemistries, J. Chem. Theory Comput. 6 (2010) 2872–2887.
[50] J.W. Ochterski, G.A. Petersson, J.A. Montgomery, A complete basis set model chemistry. V. Extensions to six or more heavy atoms, J. Chem. Phys. 104 (1996) 2598–2619.
[51] J.R. Barker, T.L. Nguyen, J.F. Stanton, C. Aieta, M. Ceotto, F. Gabas, T.J.D. Kumar, C.G.L. Li, L.L. Lohr, A. Maranzana, N.F. Ortiz, J.M. Preses, J.M. Simmie, J.A. Sonk, P.J. Stimac, MultiWell-2019 Software Suite, (2019).
[52] A.M. Mebel, M.C. Lin, Prediction of Absolute Rate Constants for the Reactions of NH_2 with Alkanes from ab Initio G2M/TST Calculations, J. Phys. Chem. A. 103 (1999)

2088–2096.
[53] Y. Guan, R. Liu, J. Lou, H. Ma, J. Song, Computational investigation on the reaction of dimethyl ether with nitric dioxide. II. Detailed chemical kinetic modeling, Theor. Chem. Acc. 139 (2020) 1–12.
[54] K.P. Shrestha, S. Eckart, A.M. Elbaz, B.R. Giri, C. Fritsche, L. Seidel, W.L. Roberts, H. Krause, F. Mauss, A comprehensive kinetic model for dimethyl ether and dimethoxymethane oxidation and NO_x interaction utilizing experimental laminar flame speed measurements at elevated pressure and temperature, Combust. Flame. 218 (2020) 57–74.
[55] Q.S. Li, R.H. Lü, Direction Dynamics Study of the Hydrogen Abstraction Reaction $CH_2O + NH_2 \rightarrow CHO + NH_3$, J. Phys. Chem. A. 106 (2002) 9446–9450.
[56] J.T. Jodkowski, E. Ratajczak, K. Fagerström, A. Lund, N.D. Stothard, R. Humpfer, H.-H. Grotheer, Kinetics of the cross reaction between amidogen and methyl radicals, Chem. Phys. Lett. 240 (1995) 63–71.
[57] M. Votsmeier, S. Song, D.F. Davidson, R.K. Hanson, Sensitive detection of NH_2 in shock tube experiments using frequency modulation spectroscopy, Int. J. Chem. Kinet. 31 (1999) 445–453.
[58] P. Glarborg, C.S. Andreasen, H. Hashemi, R. Qian, P. Marshall, Oxidation of methylamine, Int. J. Chem. Kinet. 52 (2020) 893–906.
[59] D.G. Goodwin, H.K. Moffat, R.L. Speth, Cantera: An Object-oriented Software Toolkit for Chemical Kinetics, Thermodynamics, and Transport Processes. Version 2.3.0, (2017).
[60] S. Gersen, N.B. Anikin, A. V. Mokhov, H.B. Levinsky, Ignition properties of methane/hydrogen mixtures in a rapid compression machine, Int. J. Hydrogen Energy. 33 (2008) 1957–1964.
[61] B.W. Weber, C.J. Sung, Comparative autoignition trends in butanol isomers at elevated pressure, Energy and Fuels. 27 (2013) 1688–1698.
[62] G. Mittal, M.P. Raju, C.J. Sung, CFD modeling of two-stage ignition in a rapid compression machine: Assessment of zero-dimensional approach, Combust. Flame. 157 (2010) 1316–1324.
[63] R.D. Büttgen, T. Raffius, G. Grünefeld, H.J. Koß, A. Heufer, High-speed imaging of the ignition of ethanol at engine relevant conditions in a rapid compression machine, Proc. Combust. Inst. 37 (2019) 1471–1478.
[64] C.K. Westbrook, Chemical kinetics of hydrocarbon ignition in practical combustion systems, Proc. Combust. Inst. 28 (2000) 1563–1577.